Journal of Hydrology 583 (2020) 124616

Contents lists available at ScienceDirect

Journal of Hydrology

journal homepage: www.elsevier.com/locate/jhydrol

Research papers

Understanding dynamics of groundwater flows in the Mississippi River Delta

An Li[a], Frank T.-C. Tsai[b,*]

[a] Department of Civil and Environmental Engineering, Louisiana State University, Baton Rouge, LA 70803, USA
[b] Department of Civil and Environmental Engineering, Louisiana State University, 3255 Patrick F. Taylor Hall, Baton Rouge, LA 70803, USA

ARTICLE INFO

This manuscript was handled by Peter K. Kitanidis, Editor-in-Chief, with the assistance of Todd C.C. Rasmussen, Associate Editor

Keywords:
Mississippi River Delta
Groundwater
Surface water
Modeling
Surface-groundwater interactions

ABSTRACT

Groundwater is a major component of the water cycle in the river-deltaic environment. However, the dynamics of groundwater flows in the river delta remains an open question owing to the complexities in the hydrologic and geological settings. This study employed a hydrogeological modeling approach to investigate groundwater dynamics in the Mississippi River Delta (MRD). A detailed groundwater model for the top 50 m of the MRD was constructed from the Head of Passes (RK 0) to Jesuits Bend (RK 108) using geotechnical borings and topo-bathymetric maps. Mississippi River stage and tide stage data were the key hydrologic data, which reflect hydrologic forcing (floods, storms, and hurricanes) to the groundwater system. By investigating the 2012 hydrologic year, the study presents several intriguing findings. Groundwater discharge and recharge rates to the river and surrounding bays were estimated 3 or 4 orders of magnitude smaller than Mississippi River discharge rate to the Gulf of Mexico. Nevertheless, the model showed strong surface-groundwater interactions controlled by local hydraulic gradient at the river and bay interfaces during severe hydrologic events. Specifically, during Hurricane Isaac pore water pressure was estimated 4–6 times higher than the normal condition and peak groundwater recharge was reached due to storm surges. Peak groundwater discharge sharply occurred a few days later after the hurricane passed. The study found such a dramatic change in surface-groundwater interactions was due to quick surface water receding and delayed groundwater response. As a consequence, more areas are likely exposed to harmful high pore water pressure and low factor of safety condition, which would destabilize sediments, enhance erosion, and compromise safety of coastal infrastructures such as the ring levees.

1. Introduction

A river delta is a landform created by deposition of riverine sediments as a river enters another body of water, such as ocean and lake. (Reading, 1978). In the coastal area, a river delta is normally entrenched by the river and surrounded by interdistributary bays, and tends to be aerially extensive and low-relief. Groundwater is a major component in the river-deltaic environment. Fig. 1 is a conceptual diagram depicting hydrogeological architecture and surface-groundwater interactions. A river-deltaic groundwater system is composed of confining layers and aquifers. Groundwater can interact with surface water through rivers, interdistributary bays, canals, and drains. Groundwater can also interact with atmospheric waters through precipitation and evapotranspiration. Groundwater plays an important role in biogeochemical processes via influencing water quality, nutrient flux (Chen et al., 2007; Debnath and Mukherjee, 2016; Liu and Mou, 2016), and vegetation structure (Fan et al., 2011). However, dynamics of groundwater flows in the river-deltaic environment remains an open question due to complexities in river-deltaic stratigraphy and hydrology. River-deltaic stratigraphy is formed under fluvial, deltaic and coastal processes; and river-deltaic hydrology involves frequent disturbance from floods, storms, and hurricanes. Nevertheless, groundwater flow is often overlooked in the river-deltaic environment because of rich low-permeability silty and clayey sediments where groundwater flow is less important. As a matter of fact, the river-deltaic system also contains a large volume of sandy sediments placed at depth as bar-finger sands or buried near surface as crevasse splay deposits (Fisk, 1961; Welder, 1955). These sandy deposits are favorable places for surface-groundwater interactions in the river-deltaic environment (Coleman et al., 2016; Kolker et al., 2013; Sawyer et al., 2015).

In this study, we investigate the dynamics of groundwater flows in the Mississippi River Delta (MRD). The MRD is the river delta formed at the confluence of the Mississippi River with the Gulf of Mexico (Fig. 2). The modern Mississippi River Delta Plain, formed in the past ~7500 years, consists of multiple subdeltas: Maringouin, Teche, St. Bernard, Lafourche, Plaquemines-Balize, and Atchafalaya-Wax Lake (Coleman, 1988). Development of a subdelta generally follows the delta-cycle which consists of a river-dominated regressive phase and a

* Corresponding author.
E-mail addresses: ali7@lsu.edu (A. Li), ftsai@lsu.edu (F.T.-C. Tsai).

https://doi.org/10.1016/j.jhydrol.2020.124616
Received 26 August 2019; Received in revised form 11 November 2019; Accepted 21 January 2020
Available online 24 January 2020
0022-1694/

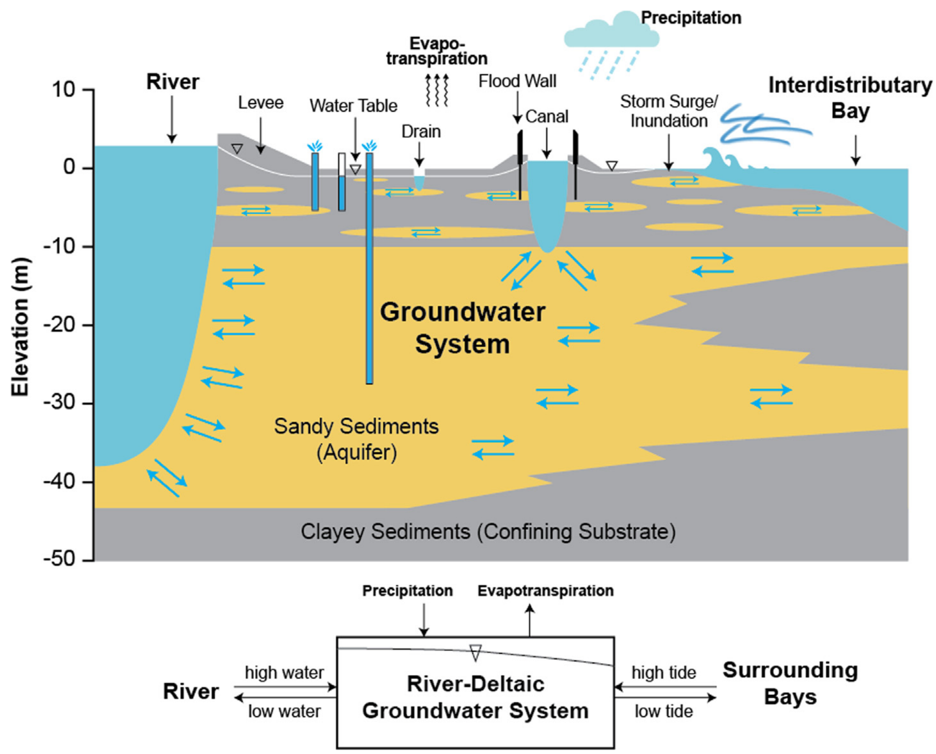

Fig. 1. A conceptual diagram of the hydrogeological architecture and groundwater-surface water interactions in the river-deltaic environment.

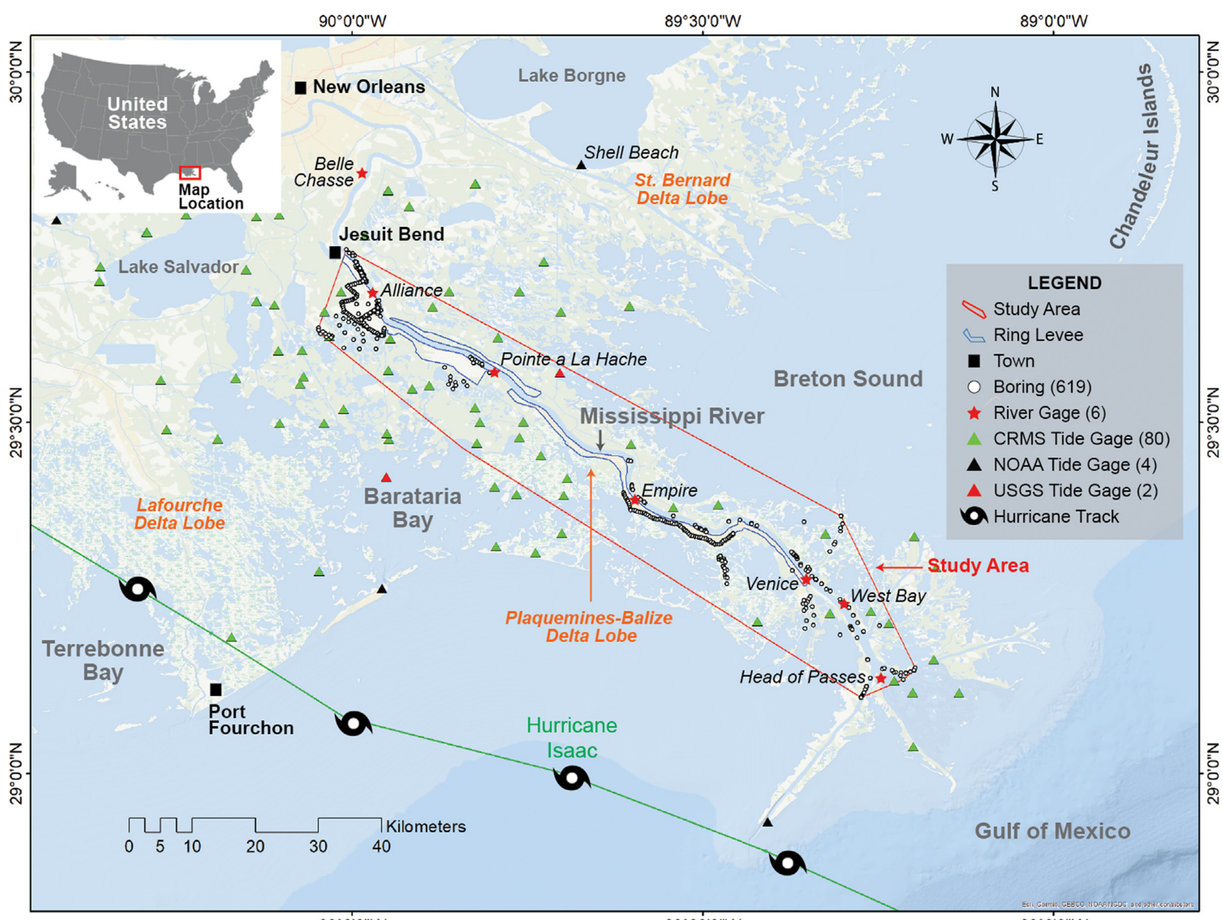

Fig. 2. Map of the study area with locations of the model domain, river gages, tide gages and the track of the 2012 Hurricane Isaac. Basemap source: Esri ArcMap.

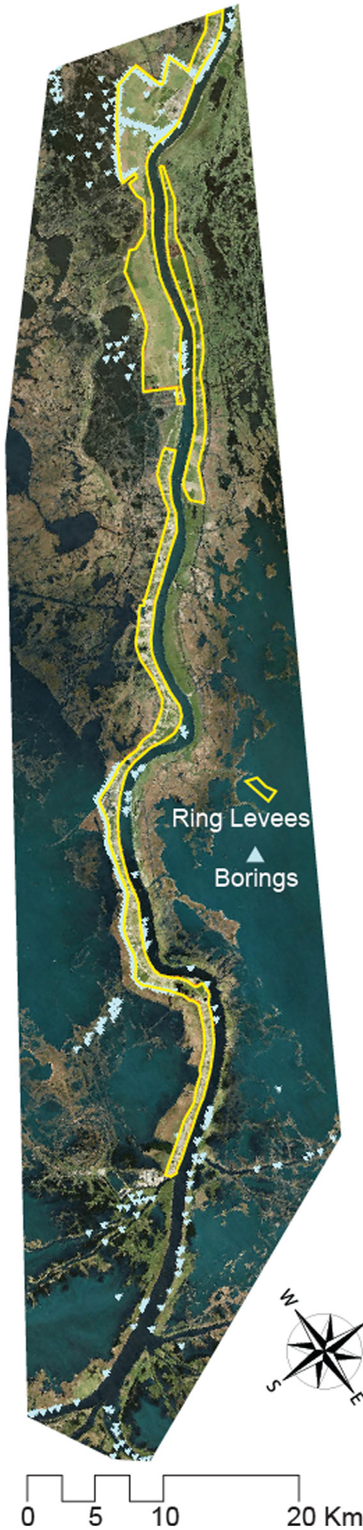

Fig. 3. Aerial image of the study area with locations of the ring levees and geotechnical borings (map source: Esri).

marine-dominated transgressive phase (Roberts, 1997). From top to bottom, the stratigraphy of a river delta normally features a silty-clayey delta plain, sandy distributary mouth bars, silty delta front deposits, and clayey prodelta deposits (Frazier and Osanik, 1969).

The MRD is one of the largest delta systems in the world (Milliman and Meade, 1983). The delta system is socioeconomically imperative to Louisiana and the United States. However, the delta system has been degrading and suffering from a high rate of land loss, which threatens coastal communities, industries, wildlife and infrastructures (Allison et al., 2016; Day and Giosan, 2008; Törnqvist and Meffert, 2008). Fifty billion U.S. dollars of coastal protection and restoration projects have been planned to cope with the land loss problem and to promote sustainability for the MRD and adjacent regions (CPRA, 2012, 2017). Many studies were conducted on the MRD, aiming at understanding the river-deltaic system (Bentley et al., 2016; Chamberlain et al., 2018) and providing insights for coastal restoration (Allison et al., 2012; Day et al., 2007; Meselhe et al., 2016; Xu et al., 2019).

Many previous groundwater related studies in the MRD were conducted in the context of submarine groundwater discharge (SGD), which refers to seaward flow or discharge of water from aquifers to oceans (Burnett et al., 2006). Researchers used geochemical tracers to assess groundwater fluxes in the near-shore marine environment (Cable et al., 1996; Kim, 2016; Krest et al., 1999; McCoy et al., 2007; Moore and Krest, 2004), and to identify flow pathways for the SGD (Kolker et al., 2013). Flow rates from 0.1 to 2.5 cm/day were reported in the coastal area along the MRD (Kim, 2016). The tracer method can be used to detect groundwater discharge at measurement locations and estimate discharge rates. However, it is still challenging to use this method to evaluate the dynamics of groundwater flows in a coastal groundwater system that involves multiple aquifers, and that shows significant spatial and temporal variabilities (Burnett et al., 2006). Moreover, the SGD only accounts for one direction of groundwater flow. Landward flow or recharge of water from oceans to aquifers, have seldom been discussed in the MRD.

This study attempts to fill in the knowledge gap in how the hydrologic and hydrogeological settings influence groundwater flows in the MRD. Major research questions in this study include: (1) where groundwater and surface water (river and bay waters) interact in a river-deltaic system? (2) how groundwater head and groundwater flow respond to seasonal flood, storm, and hurricane events? and (3) what role groundwater may play in the coastal sustainability?

Past studies have employed groundwater models to address some of these questions. Thompson et al. (2007) developed a large-scale conceptualized groundwater model up to depth 5 km to evaluate groundwater-seawater circulation in the continental shelf of Louisiana. The study concluded that no substantial terrestrial-origin groundwater discharge exists on the continental shelf. On the contrary, O'Connor and Moffett (2015) developed a small-scale groundwater model to study surface-groundwater interactions in a young prograding delta island within the Wax Lake Delta west of the MRD. The study found that intensity and direction of the groundwater flow are controlled by hydraulic gradients at surface water-groundwater interfaces. However, both groundwater models were hydrogeologically simple and did not capture the heterogeneity in the depositional environment of sandy, silty, and clayey sediments for a river-deltaic system.

This study developed a more detailed groundwater model to address the aforementioned questions. In this study, an integrated groundwater model was constructed along Mississippi River from the Head of Passes (RK, river kilometer 0) to Jesuits Bend (RK 108). The model focuses on the topmost 50 m of the river delta. Many emerging datasets (geotechnical borings, topobathymetric maps, river and tide gauges, etc.) were used to construct the model. Geotechnical borings were used to construct a stratigraphy model, which serve as the structure of the groundwater model. Topobathymetric maps were used to determine the surface of the groundwater model. River and tide gauges were used to determine flood, storm, and hurricane events to the model boundary conditions.

2. Study area

The study area shown in Fig. 2 covers a large portion of the Plaquemines-Balize delta lobe, which is formed between Lafourche delta lobe to the southwest and St. Bernard delta lobe to the northeast. The area is about 1800 km^2, with maximum length of ~100 km, and maximum width ~20 km. The area is bounded by Barataria Bay to the northwest, Breton Sound to the east, and Gulf of Mexico to the south and southwest. As shown in Fig. 3, the upper half of the area mainly consists of a trunk river channel, natural levees, tidal marshes, and impounding lakes. The lower half of the area mainly consists of the trunk river channel, splay channels, broken tidal marshes and open waters. Residential and business areas are protected by the ring levees along Mississippi River.

Due to its subtropical latitude, low lying topography, and proximity to the Gulf of Mexico, southeastern Louisiana has a humid subtropical climate. The study area has long, hot, and humid summers, and short and mild winters. Annual average temperature is about 21 °C. Annual average precipitation is about 1600 mm. The area has about 110 days of precipitation per year (National Climatic Data Center, 2018). The MRD is often affected by hydrologic events, such as river floods and tropical cyclones. The lowlands are very vulnerable to major hurricanes; and the area is also prone to frequent thunderstorms, especially in summer months. Hurricane Katrina and Hurricane Isaac are the two most recent major hurricanes that made landfall within 30 km of the study area. Hurricane Katrina was a Category 5 hurricane that made landfall near Buras-Triumph, Louisiana in August 2005, causing more than 1800 fatalities, and 125 billion dollars of property damage (Knabb et al., 2005). Hurricane Isaac was a Category 1 hurricane that made landfall near the southwest of the Mississippi River mouth in August 2012, causing 41 fatalities and 3 billion dollars of property damage (Berg, 2013).

3. Hydrologic data and hydrologic events in 2012

This study investigates groundwater dynamics associated with hydrologic forcing between November 1, 2011 and October 31, 2012. Daily river stage data were collected from stations at Alliance, Pointe a La Hache, Empire, Venice, West Bay, and Head of Passes (Fig. 2). The river gage data are maintained by the U.S. Army Corps of Engineers (USACE) (USACE, 2018). Fig. 4a shows hydrographs for the six stations. The vertical datum for all river stages is the North American Vertical Datum of 1988 (NAVD 88). This period includes three seasonal Mississippi River floods before May 2012, Tropical Storm Debby in June 2012, and Hurricane Isaac in August 2012. Each of the three floods lasted about one and a half months. Crest stages were over 1.5 m at northern stations. Tropical Storm Debby was formed on June 23, 2012 from a trough of low pressure and made landfall in Florida's Big Bend region on 26 June 2012 (Kimberlain, 2013). River stages were raised by storm surges and were above 1 m at northern stations.

Hurricane Isaac caused dramatic water level increase in all stations in Mississippi River between August 21 and September 1, 2012. Hurricane Isaac was a Category 1 hurricane prior to making two landfalls in southeastern Louisiana (Berg, 2013). Fig. 2 shows the hurricane track. The first landfall was made at the Southwest Pass at the mouth of the Mississippi River around 0000 Coordinated Universal Time (UTC) 29 August. The second landfall was made west to Port Fourchon, Louisiana, around 0800 UTC 29 August (Berg, 2013). The hurricane slowed down while approaching the coast of Louisiana. The slow movement prolonged the strong wind, high storm surges, and heavy rainfall along the coast. Strong easterly wind caused large storm surges along the eastern shore of the Plaquemines-Balize and St. Bernard delta lobes, and the western shore of Lake Borgne (Guy et al., 2013). The storm surges elevated water level in Mississippi River more than 1.5 m at all stations and more than 2 m at northern stations.

The hydrologic events in 2012 set an ideal groundwater study based upon two distinct hydrologic episodes on the MRD. One hydrologic episode is the hydrologic loading from seasonal Mississippi River floods, which usually end before June every year (Junk et al., 1989). The other hydrologic episode is the hurricane season, which starts June every year (Larson et al., 2005). Another possible hydrologic episode that both Mississippi River floods and hurricanes occur at the same time never happened before. Hurricane Barry in July 2019 was a close one, but Barry made a landfall about 210 km west of the study area when it became a Category 1 hurricane (National Weather Service, 2019).

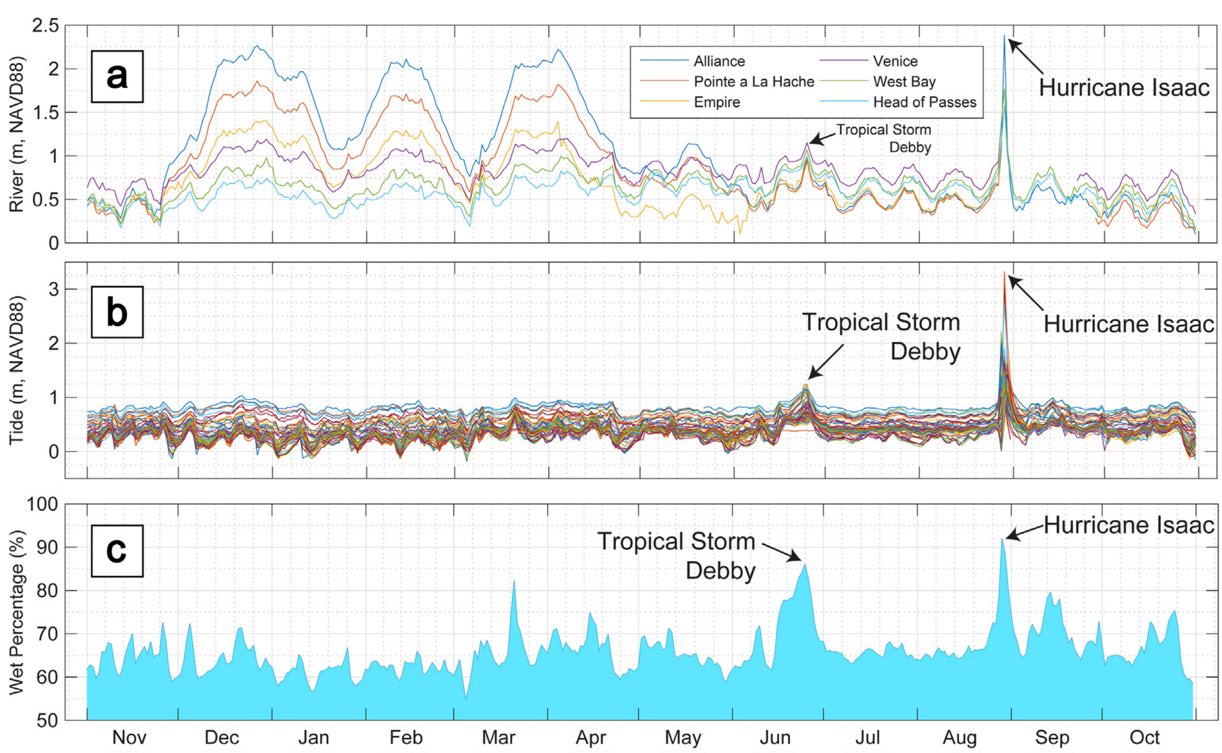

Fig. 4. (a) Water levels at river gauges (USACE, 2018); (b) water levels at tide gauges (CPRA, 2018; NOAA, 2018a,b); and (c) percentage of tide cells that are wet. Locations of river and tide gauges are shown in Fig. 2.

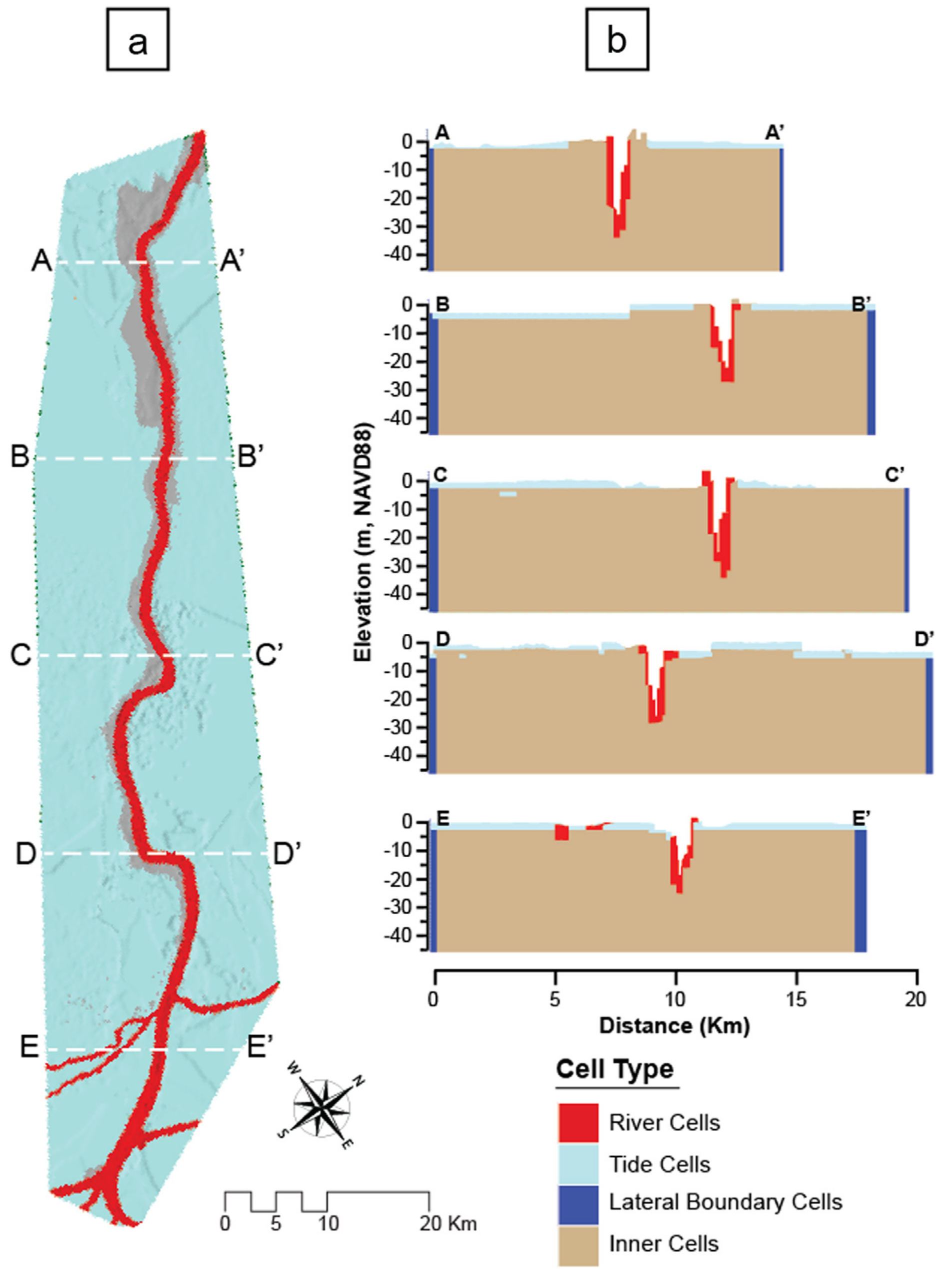

Fig. 5. Model cells for boundary conditions: (a) plan view, and (b) cross sections.

Tidal stage data were collected from 86 tide gages in and around the study area (Fig. 2). Eighty (80) gages were from CPRA's Coastwide Reference Monitoring System (CPRA, 2018), four (4) gages were from NOAA's Tides and Currents database (NOAA, 2018a,b), and two (2) gages were from USGS' National Surface-Water database (USGS, 2018). All water level data were adjusted to the NAVD 88 datum using NOAA's vertical datum transformation tool (NOAA, 2018a,b). Fig. 4b shows the daily water levels from November 1, 2011 to October 31, 2012 for all 86 tide gages. Normal tidal water levels in all tide gages are generally between 0 m and 1 m NAVD 88. The seasonal Mississippi River floods had minimum influence on tidal water levels. However, tidal water levels were elevated by Tropical Storm Debby and Hurricane Isaac. Tropical Storm Debby raised tidal water level over 1 m at several gages. Strong storm surges from Hurricane Isaac caused a spike in all tide gages. Some tide gages experienced more than 3 m water levels.

Tidal stage data were interpolated to determine boundary conditions for the model's lateral boundaries. Moreover, tidal stage data were also interpolated to determine surficial boundary conditions that reflect open water and inundated areas in the model domain and water levels above land surface. Inundations increase groundwater recharge from land surface.

In general, more than 60% of the model domain was under water during the normal condition (no Mississippi River high water, no severe storms, and no hurricanes) as shown in Fig. 4c. Due to the low relief topography, small fluctuations in tides can substantially alter the extent of the inundated areas. There is a spike on March 21, 2012 that more than 80% of the model domain was under water. This was caused by a trough of low pressure that slowly moved eastwards and generated severe thunderstorms and outbreak of tornados across southeast Louisiana (Storm Prediction Center, 2012). Tropical Strom Debby caused more than 85% of the model domain to be inundated. Hurricane Isaac caused more than 90% of the model domain to be inundated.

4. Methods

4.1. Construction of stratigraphy model

Geotechnical data were used to determine sediment types and build a stratigraphy model for the study area. 619 borings were collected from the USACE, USGS, and CPRA. The boring sites are along the river levees and on marshlands (Fig. 2). Each boring records sediment types and corresponding elevations with respect to the NAVD 88. Sediment types were classified by the Unified Soil Classification System (USCS) (ASTM, 2017), which include poorly-graded sand (SP), silty sand (SM), clayey sand (SC), silt (ML), elastic silt (MH), low-plasticity clay (CL), high-plasticity clay (CH), organic clay (OH), and peat (PT).

Distribution of sediment types for the study area was estimated at 0.3 m (1 ft) intervals from 3 m to −46 m NAVD 88. The model was discretized into 161 layers. Each layer has 44,810 cells. Cell size is 200 m by 200 m. A multiple indicator natural neighbor interpolation (MINN) method was used to obtain layer-wise distribution of sediment types for each layer. The MINN method is based on the natural neighbor interpolation (NN) method (Sibson, 1980; Sibson, 1981; Tsai et al., 2005). Indicator values of the 9 sediment types were calculated by the MINN method at a location. The final sediment type for the location was determined by the highest indicator value. Then, the 161 layers were stacked and upscaled into a three-dimensional stratigraphy model by merging adjacent vertical cells that have the same sediment type (Li et al., 2019a; Li et al., 2019b). The upscaling procedure resulted in a 25-layer stratigraphy model with a total of 1,120,250 cells. We will discuss the stratigraphic modeling results in the Results and Discussion section.

A topobathymetric map was used to determine the relief of the stratigraphy model and later the groundwater model. The topobathymetric map was generated by merging a digital elevation model of New Orleans (Love et al., 2010a) and a digital elevation model of Southern Louisiana (Love et al., 2010b). Both of the data sets have a resolution of 1/3 arc-second (approximately 10 m) and vertical datum NAVD 88.

4.2. Groundwater model development

The structure of a groundwater model was built based upon the stratigraphy model. This study used MODFLOW-USG (Panday et al., 2017) to simulate groundwater flow in the MRD. MODFLOW-USG uses a generalized control volume finite difference (CVFE) approach to solve groundwater flow equations (Narasimhan and Witherspoon, 1976).

The groundwater model simulated daily groundwater head and groundwater flow from November 1, 2011 to October 31, 2012. There were 366 daily time steps. As groundwater head distribution on November 1, 2011 represents the groundwater condition without severe hydrologic events for a month, groundwater head in the first time step was simulated under the steady-state condition. Groundwater head in other time steps was simulated under the transient condition. The daily time step was used, instead of hourly time step, in the simulation to understand groundwater dynamics on events that last for days (e.g. neap/spring tides, storms, and hurricanes) or months (e.g. floods) in a time frame of a hydrologic year.

There are three types of boundaries in the model as shown in Fig. 5. These boundaries correspond to the surface-groundwater interfaces. The river boundary is at the interface between Mississippi River and the subsurface and was identified as river cells in the model. The tide boundary is at the interface between surrounding bays (including inundated areas) and the subsurface and was identified as tide cells. The lateral boundaries are the model outer boundaries, shown in Fig. 5b, which are influenced by tides. The cross sections show that Mississippi River incises 20 m to 40 m into the subsurface. Other non-boundary cells are inner cells in the model domain.

A general head boundary condition was assigned to the three types of boundaries, which characterizes a head-dependent flux across a material at the boundary as follows

$$Q = K'A(H - h_b),$$

where Q is the flow rate [m^3/day] across the boundary material, K' is the hydraulic conductivity per unit width of the boundary material [1/day], A is the cross-sectional area of the boundary material perpendicular to the flow [m^2], H is the hydraulic head of a boundary forcing term [m], and h_b is the groundwater head at the boundary [m]. $K'A$is the hydraulic conductance [m^2/day].

To assign hydraulic head at the river boundary, water levels at the 6 river gauges (Fig. 4a) were interpolated to all river cells according to river kilometers. To assign hydraulic head at the tide boundary, tidal stages at the 86 tide gauges (Fig. 4b) were interpolated to all tide cells. Special attention was paid to determining tide cells for the inundated areas because the inundated areas changed over time. “Wet and dry” condition for surficial cells was taken care by comparing tidal water level to land elevation. For the lateral boundaries, interpolated tidal stages at the model boundary were used to assign the boundary values.

Surficial groundwater recharge from precipitation and groundwater loss from evapotranspiration were not directly considered in the model because the majority of the model domain is under water. The river and tidal water levels have taken precipitation and evaporation into consideration.

As a result, groundwater storage gain or loss in the MRD depends on groundwater interactions with the Mississippi River and the surrounding bays, and groundwater fluxes through the lateral boundaries. A simplified water balance equation is

$$\Delta S = I_{river} + I_{bays} + I_{lateral} - O_{river} + O_{bays} + O_{lateral},$$

where $\Delta S$is the storage change [m^3], I is the inflow [m^3], and O is the outflow [m^3]. The inflow and outflow terms at the boundaries are determined by the groundwater model through water budget analysis.

4.3. Model parameter sensitivity and uncertainty analyses

Model parameters include hydraulic conductivity (K), specific storage (S_y), and specific yield (S_s) for the 9 sediment types and $K'$for the river, tide, and lateral boundaries. In total, there are 30 parameters need to be determined. Unfortunately, there is no groundwater data available in the study area for model calibration. Instead, sensitivity analysis was conducted to evaluate how model parameters affect groundwater recharge rates from the river, tide, and lateral boundaries. Table 1 lists the range of parameter values from the literature for sensitivity analysis. Sensitivity analysis was carried out for the thirty parameters.

A composite scaled sensitivity (CSS) method (Hill et al., 1998) was used to identify the most sensitive parameters among all parameters. To calculate the CSS, the total groundwater recharge flowrate for the k^{th} value of parameter $p_j^{(k)}$ was calculated by

$$Q^{(k)} = \sum_{t=1}^{T} \sum_{i=1}^{N} Q_{it}^{(k)},$$

where $Q_{it}^{(k)}$ is the flowrate at boundary cell i at time t with respect to parameter $p_j^{(k)}$. Then, the CSS value for the k^{th} value of parameter $p_j^{(k)}$ was calculated by

$$CSS_j^{(k)} = \frac{\partial Q^{(k)}}{\partial p_j^{(k)}} \frac{p_j^{(k)}}{\sigma_Q},$$

where σ_Q is the standard deviation of the total groundwater recharge flowrate Q. The final CSS value with respect to parameter p_j was calculated as:

$$CSS_j = \sqrt{\frac{1}{M} \sum_{k=1}^{M} [css_j^{(k)}]^2},$$

where M is the sample size of parameter $p_j^{(k)}$.

The CSS ranked the model parameters from the most sensitive

Table 1
Ranges of parameter values.

USCS	Sediment Type	K (m/d)[1,2,3,4,5]	S_s (1/m)[6,7,8]	S_y[6,9,10]
SP	Poorly graded sand	3 – 300	4.57×10^{-6}–9.45×10^{-6}	0.15–0.35
SM	Silty sand	1–90	1.19×10^{-5}–1.89×10^{-5}	0.10–0.28
SC	Clayey sand	0.1–10	4.57×10^{-5}–9.45×10^{-5}	0.07–0.20
ML	Lower plasticity silt	0.0001–1	6.1×10^{-5}–1.07×10^{-4}	0.03–0.19
MH	High plasticity silt	0.0001–1	6.1×10^{-5}–1.07×10^{-4}	0.03–0.19
CL	Low plasticity clay	0.00004–0.004	1.19×10^{-4}–2.38×10^{-4}	0.0001–0.12
CH	High plasticity clay	0.00004–0.004	2.38×10^{-4}–1.89×10^{-3}	0.0001–0.12
OH	High plasticity organics	0.00004–0.009	2.38×10^{-4}–1.89×10^{-3}	0.0001–0.12
PT	Peat	1–780	8×10^{-7}–2×10^{-6}	0.2–0.6

[1] Freeze and Cherry (1979)
[2] Robertson and Cabal (2015)
[3] Leonards (1962)
[4] Hogan et al. (2006)
[5] Thompson et al. (2007)
[6] Younger (1993)
[7] Domenico and Mifflin (1965)
[8] Batu (1998)
[9] Johnson (1967)
[10] Letts et al. (2000)

parameter to the least sensitive parameter. Then, uncertainty analysis was carried out by sampling the top most sensitive parameters using the Latin Hypercube Sampling (LHS) method (Helton and Davis, 2003). Ranking of the sensitivities will be discussed in the Results and Discussion section. Thirty (30) sets of realizations were generated using the LHS method. Simulations were carried out using these sets of sampled parameters. Model results from these simulations will be discussed later.

4.4. Factor of safety (FS) calculations

Factor of Safety (FS) is a commonly used measure for the potential concern of sand boils and uplifting (Harr, 1962; USACE, 1993; FEMA, 2015). This study adopts the FS as an indicator to imply sediment stability in the river-deltaic setting. FS is estimated from a ratio of effective weight of the soil to net pressure head against the top stratum. A factor of safety greater than 1.5 is preferred. FS is also referred as the ratio of the critical upward hydraulic gradient to in-situ upward hydraulic gradient (USACE, 1993):

$$FS = \frac{i_c}{i},$$

where i_c is the critical hydraulic gradient and i is the hydraulic gradient across the top stratum. The hydraulic gradient across the top stratum was derived from the groundwater model. Since the top stratum is not homogeneous, transformed thickness in terms of clay sediments was calculated for the top stratum based on the method in (USACE, 1992). A value of 0.8 is commonly used for the critical hydraulic gradient (USACE, 1956).

5. Results and discussion

5.1. MRD stratigraphy

The emerging subsurface investigation dataset made possible for this study to estimate the spatial distribution of different sediments and to evaluate connectivity between groundwater and surface water bodies in the MRD. As shown in Fig. 6a, the surface of the MRD is dominated by estimated silty (ML and MH), clayey (CL and CH), and organic clay (OH) sediments, which form a large surficial confining layer. However, a large area of estimated sandy sediments in the middle of the MRD is exposed to land surface or directly contacts bay water. Estimated sandy sediments are also exposed to the Mississippi River channel or near the river mouth.

Silty and clayey sediments also make up the largest portion under the MRD as shown in the cross sections (Fig. 6b). Thickness of the surficial confining layer varies greatly from 0 to the entire model depth. Most of the sandy sediments (SP, SM, and SC) were deposited along and below the main Mississippi River channel and are confined by fine-grained sediments, except for those exposed to the topobathymetric surface (see cross section CC′). Some sands are interlayered by silty and clayey sediments near surface.

Sedimentological heterogeneity causes complex hydrogeological heterogeneity in the river-deltaic system (O'Connor and Moffett, 2015; Wolski and Savenije, 2006). Though the stratigraphy model shows a general clay-sand-clay layering in the MRD, the near-surface stratigraphy is complicated by sandy sediments deposited through splay channel in-fill, overbank flooding, and tributary extension (Bomer et al., 2019; Esposito et al., 2017; Kolker et al., 2013; Shen et al., 2015). These sandy sediments can serve as preferential conduits for groundwater flow and form hotspots for groundwater exchanging and mixing with river and bay waters.

5.2. Sensitivity and uncertainty analyses

Sensitivity analysis was conducted on the model parameters. The rank is shown in Fig. 7. Specific yield of CL and specific storage of SM, ML, CL, SP, and SC are the top 6 sensitive parameters. Other parameters have CSS less than 4. CL is abundant at or near the surface and SM, ML, SP, and SC are abundant and connect to the river, which makes the specific yield of CL and the specific storage of SM, ML, CL, SP, and SC the most sensitive model parameters.

Uncertainty analysis was conducted by sampling from the 6 most sensitive parameters. Thirty (30) sets of parameters were generated using the LHS method and input to the groundwater model to evaluate uncertainty. One standard deviation was used to quantify the uncertainties in flow rates and storage changes.

5.3. Groundwater-Mississippi River interactions

Groundwater recharge from or discharge to Mississippi River depends on local hydraulic gradients along the river. Fig. 8 shows the simulated mean flow rates through the river boundary with one standard deviation uncertainty from Nov. 2011 to Oct. 2012. Higher flow rates associate with higher estimation uncertainty. For non-flood and non-hurricane periods, groundwater recharge and discharge rates were

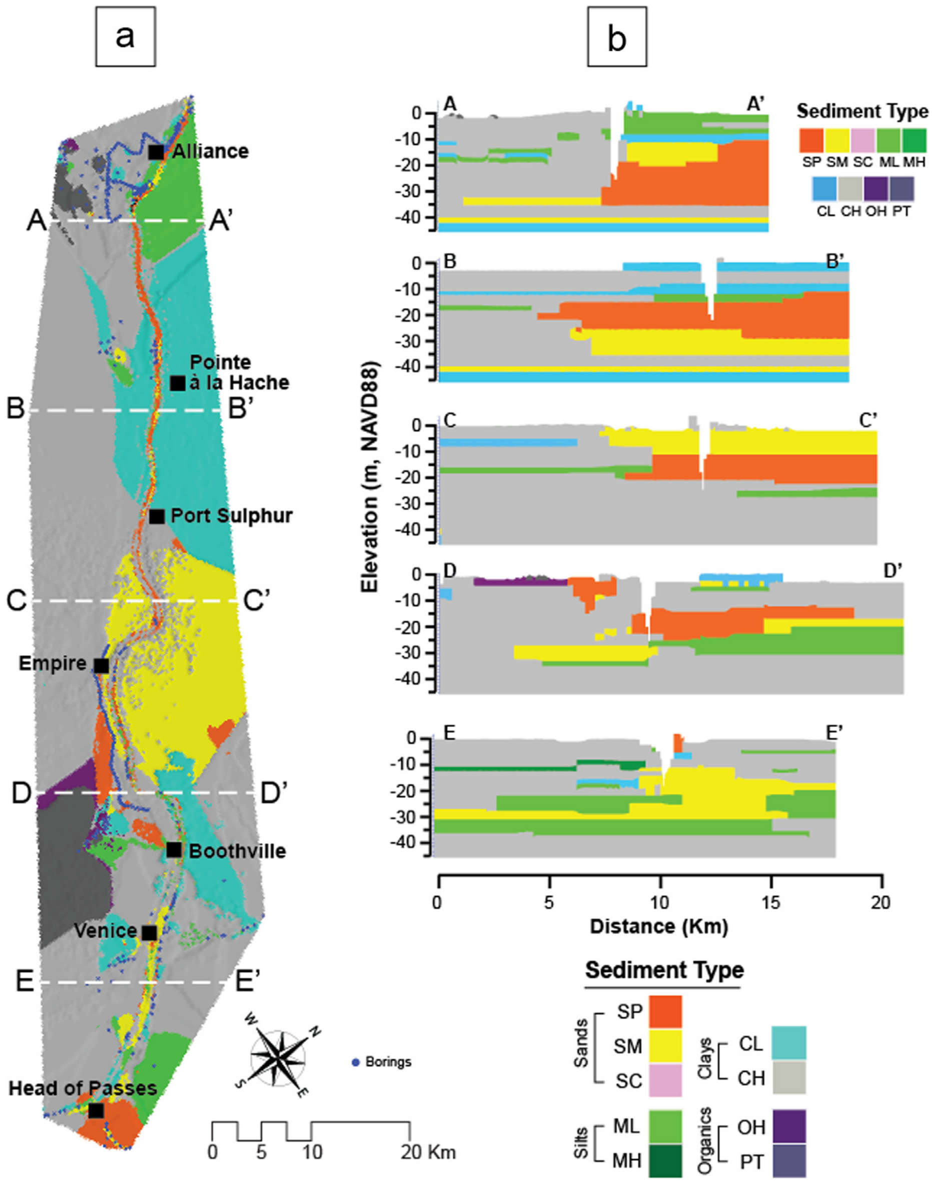

Fig. 6. (a) Top view of the stratigraphy model, and (b) cross-sections of the stratigraphy model.

estimated generally within 0.4 million m^3/day. Groundwater recharge rate could reach as high as 0.75 million m^3/day during the three flood events. Nevertheless, low groundwater discharge rate still occurred whenever river stage dropped below groundwater head during the floods. Tropical Storm Debby intensified groundwater recharge rates, which was estimated up to 0.5 million m^3/day. Storm surges by Hurricane Isaac created a sharp groundwater recharge rate, which was estimated as high as 2.5 million m^3/day, followed by a sharp groundwater discharge rate estimated around 1 million m^3/day in responding to the rapid river water drop after the hurricane passed. Comparing to the mean Mississippi River flow rate 1.145 billion m^3/day (468,000 ft^3/sec) at Belle Chasse, it is not surprising to see that the groundwater recharge and discharge rates in the MRD are very small.

This result is in agreement with a previous study in the Breton Sound (Hyfield et al., 2008) that the groundwater flow rate is significantly less than inputs from precipitation or river diversion. Moreover, dividing the estimated groundwater flux with the river channel surface area yields specific discharge between 0.1 cm/day and 1 cm/day, which is similar to the previous measurements (e.g., Kim, 2016). However, the groundwater flux estimation in this study is much less than the estimation made by some of the previous studies in the river-deltaic environment. For example, Moore and Krest (2004) concluded that groundwater fluxes on the western side of the MRD equal to 7% of the average Mississippi River discharge; and Basu et al. (2001) claimed that the groundwater flux in the Bay is approximately 19% of the total discharge in the Ganges-Brahmaputra River, Bangladesh.

5.4. Groundwater-bay interactions

Groundwater recharge from and discharge to the surrounding bays are controlled by vertical hydraulic gradients at the topobathymetric surface. As shown in Fig. 9, the groundwater system exchanges water more frequently with bays than with the Mississippi River. Processes such as spring and neap tides (Li et al., 2000) cyclically fluctuate the sea level, and thus alternate vertical hydraulic gradients recurrently. Moreover, cold fronts in the region may also contribute to the sea level fluctuation. Cold fronts normally last for 3 to 7 days and are the common weather pattern between October and April along Louisiana's coast (Chuang and Wiseman, 1983). The onshore wind during pre-frontal phase of a cold front can set up sea level along the coast (Christopher et al., 1993). And the offshore wind during the post-frontal phase can flush out water in the bay and drop sea level (Feng and Li,

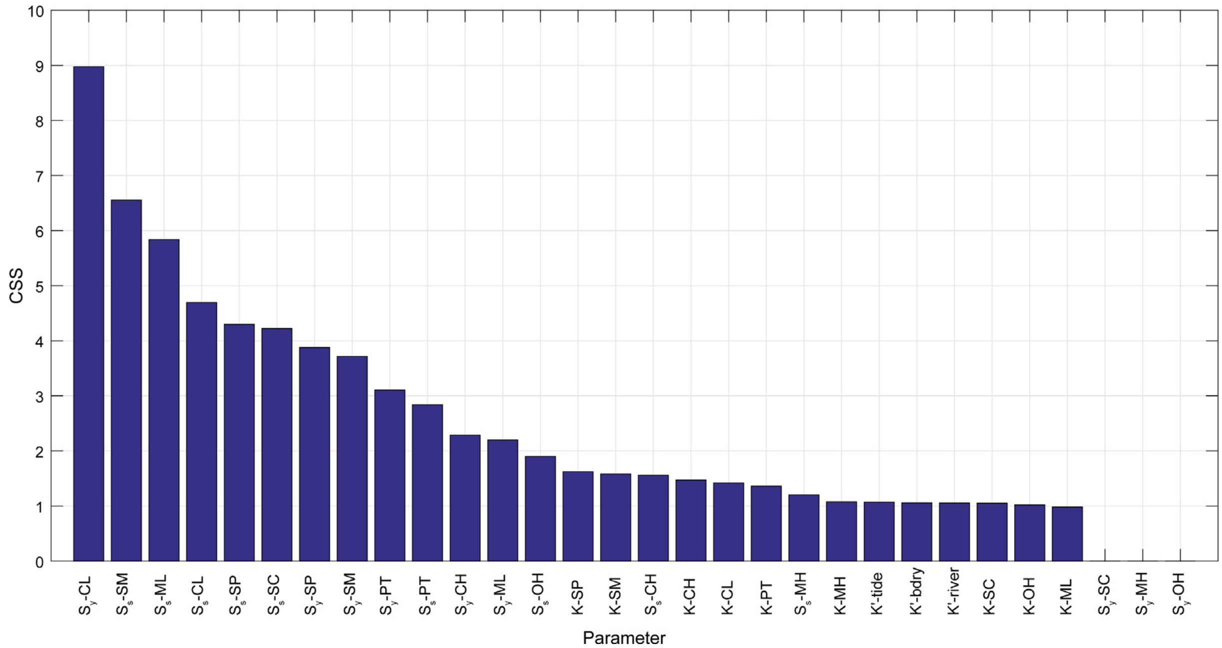

Fig. 7. CSS rank of the model parameters. S_y refers to specific yield. S_s refers to specific storage. K refers to hydraulic conductivity. K′ refers to hydraulic conductivity per unit width of the boundary material.

2010).

Groundwater recharge and discharge rates were estimated generally within 1 million m^3/day during Nov. 2011 to Oct. 2012. The three major floods had minimum impact on the groundwater-tide interactions. However, thunderstorms around March 21, 2012 (Storm Prediction Center, 2012) and Tropical Storm Debby during June 23–26, 2012 elevated sea level and intensified groundwater recharge rate estimated more than 1 million m^3/day. Storm surges by Hurricane Isaac (August 28 to September 1) significantly elevated sea level and induced sharply high groundwater recharge rate estimated about 5.6 million m^3/day, which was quickly reversed by groundwater discharge with a rate about 2 million m^3/day in responding to the sharp sea level drop.

The inundation area (Fig. 4c) is proportional to the groundwater-bay exchange rate and is the reason why groundwater-bay interactions is stronger than groundwater-river interactions in the MRD. However, the temporal change in the inundation area likely determines either groundwater recharge or groundwater discharge because groundwater head slowly responses to tides. Due to the low relief topography of the study site, frequent changes in the tidal stage can cause frequent changes in inundation patterns and direction of groundwater flow on the tidal flats (O'Connor and Moffett, 2015). The frequent changes in groundwater flow direction may lead to a tidal pumping effect (Liu et al., 2017) and recirculation of seawater, which may account for a large portion of total SGD fluxes (Santos et al., 2009). Through exchanging and mixing of groundwater and surface water, biogeochemical processes can take place to alter biogeochemistry in the river-deltaic system (Bianchi et al., 2013).

5.5. Groundwater flux across lateral boundaries

Groundwater flow across the lateral boundaries is influenced by both Mississippi River and the interdistributary bays. Fig. 10 shows that groundwater outflow dominates groundwater inflow at the lateral boundaries most of the time. This is because of the general seaward hydraulic gradient established by the relatively high Mississippi River water with respect to the interdistributary bays. However, the flow rates were estimated one order of magnitude smaller than those at the groundwater-river and groundwater-tide interfaces. The three flood events established high groundwater head around the river and pushed more groundwater out through the lateral boundaries. Most of the elevated groundwater discharge rates were estimated below 10,000 m^3/day. On the contrary, storm surges from the severe

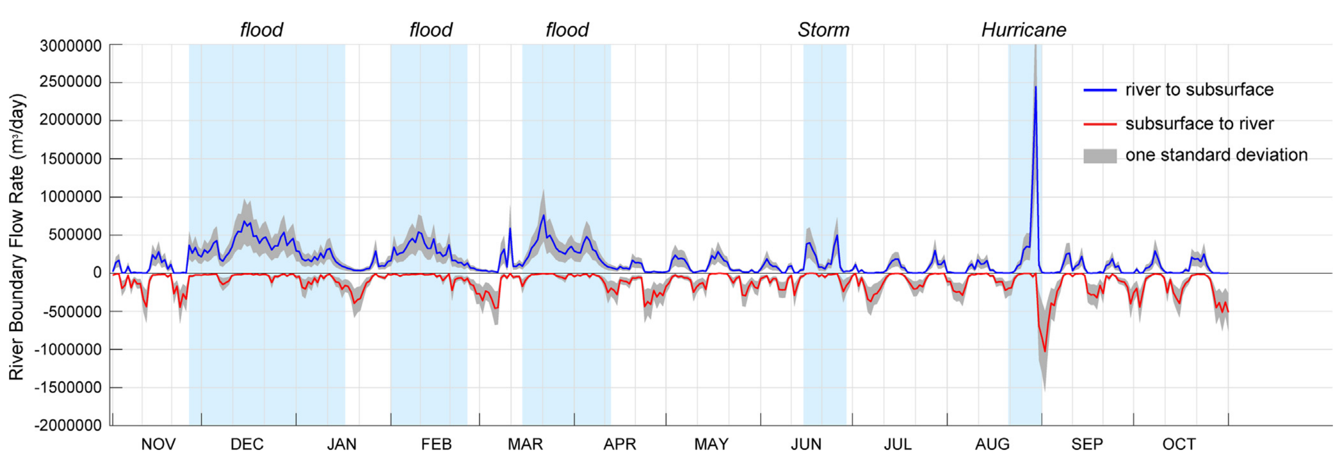

Fig. 8. Groundwater recharge and discharge flow rates at the subsurface-river boundary. Gray color represents the area of one standard deviation.

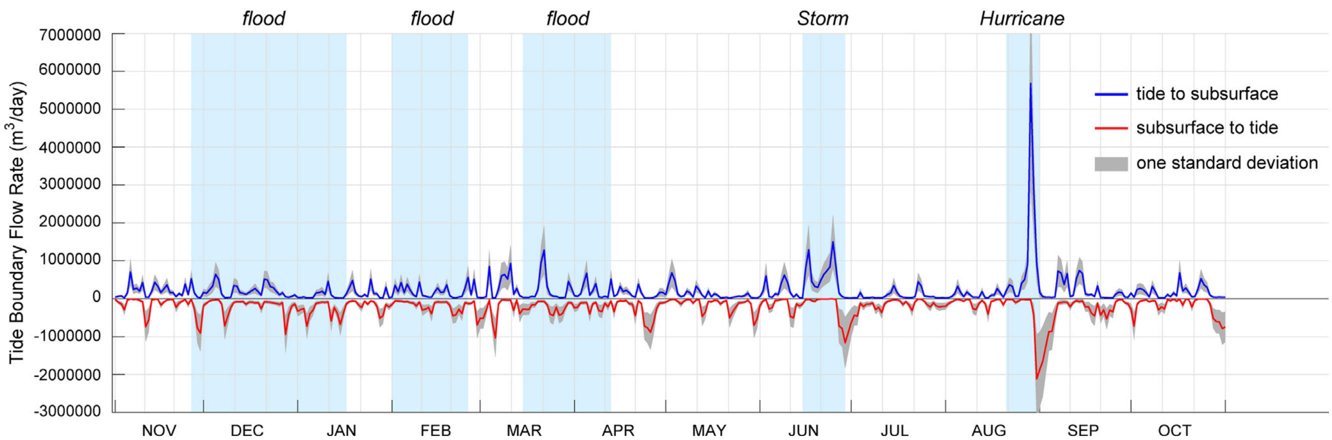

Fig. 9. Groundwater recharge and discharge flow rates at the subsurface-tide boundary. Gray color represents the area of one standard deviation.

thunderstorms in March, Tropical Storm Debby in June, and Hurricane Isaac in August increased sea level and resulted in groundwater recharge from the lateral boundaries. The peak recharge rate was estimated 34,000 m^3/day during Hurricane Isaac.

5.6. Groundwater storage variation

Groundwater storage increase or decrease in the MRD strongly associates with surface water dynamics. As shown in Fig. 11, daily groundwater storage variation was estimated within 1 million m^3, except for the storm and hurricane events. The peak daily storage gain was occurred during Hurricane Isaac, estimated nearly 7.5 million m^3, followed by the peak daily storage loss after 3 days.

Cumulative storage changes with respect to the storage on 01/11/2011 show a regular pattern that groundwater storage always increases during flood, storm and hurricane events, followed by groundwater storage recession (Fig. 11). The groundwater flow simulation started at a low river stage and the year 2012 was a wet year for the MRD. The tropical storm Debby and the Hurricane Isaac reversed the recessing trend of groundwater storage between June and September. Although floods in 2012 were smaller than 2011, the relatively higher post-flood river stage along with the storm and hurricane events in 2012 caused the groundwater system to gain around 9 million m^3 at the end of the simulation period (10/31/2012).

5.7. Groundwater head dynamics

Due to a lack of groundwater models, previous studies rarely discuss groundwater head dynamics in the river-deltaic setting. This section discusses the spatiotemporal variation of groundwater head in different hydrologic conditions in the MRD.

5.7.1. Pre-flood season condition

Groundwater head distribution on November 1, 2011 represents the groundwater condition without severe hydrologic events for a long time (say one month). Groundwater head is relatively uniform and low as shown in Fig. 12a. Groundwater head was estimated between 0.1 m and 0.7 m in most of the area. During pre-flood season, river stages and tidal stages are relatively low. Low hydraulic gradients indicate low groundwater flow exchanges with the river and the surrounding bays.

5.7.2. Groundwater response to flood peak

Groundwater head distribution on February 11, 2012 represents the groundwater condition at the crest of a flood. Groundwater head was high around the Mississippi River as shown in Fig. 12b. Groundwater head along the river and near the river mouth was estimated between 0.7 m and 2.2 m. High groundwater head was built up in the sandy deposits between elevation −10 m and −35 m and dissipated seaward. High river stage leads to high groundwater recharge. The result indicates a good hydraulic connection of the groundwater system to river water in deltaic distributary channel networks (Sawyer et al., 2015).

5.7.3. Groundwater response to storm

Groundwater head distribution on June 25, 2012 represents the groundwater condition at peak river/tidal stages caused by a tropical storm. As shown in Fig. 12c, groundwater head was estimated between 0.7 m and 1 m around the river, and between 0.1 m and 1.3 m underneath the surrounding bays. Different from the flood condition, elevated groundwater head occurred not only in deep sands between −10 m and −35 m, but also in surficial sands, for example the cross

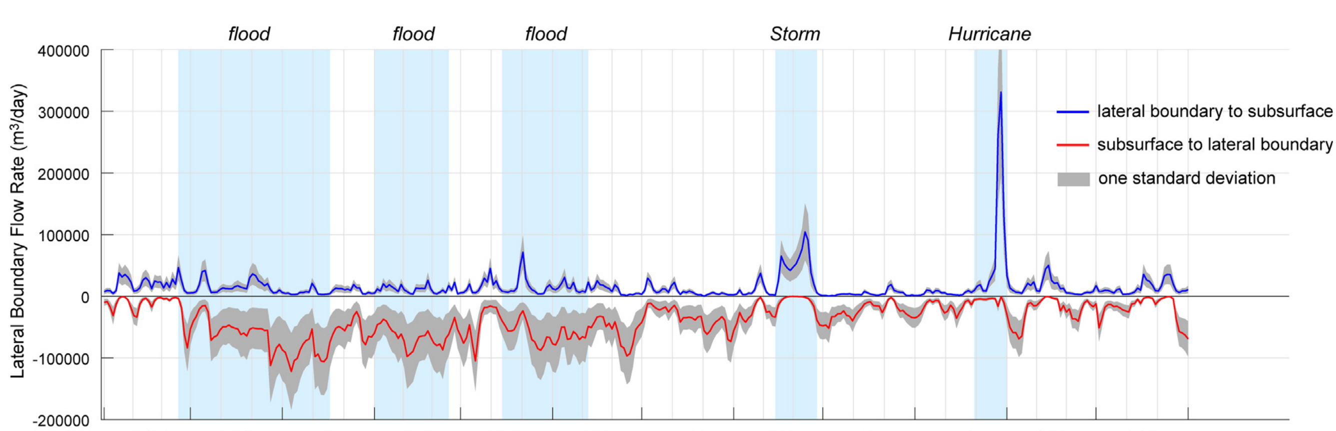

Fig. 10. Groundwater recharge and discharge flow rates at the subsurface-lateral boundary. Gray color represents the area of one standard deviation.

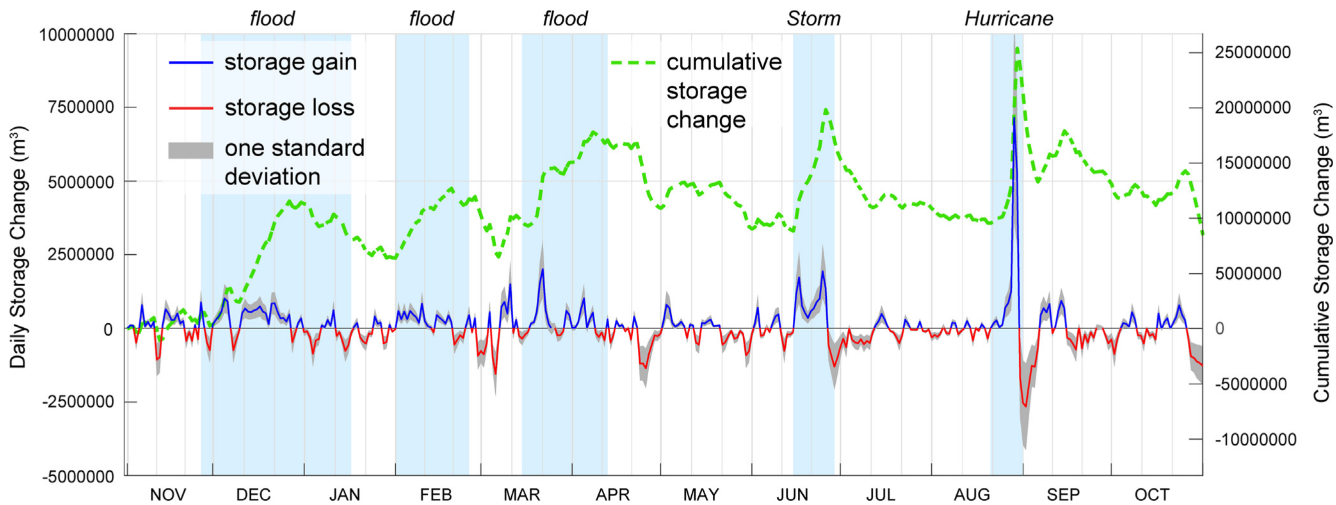

Fig. 11. Daily groundwater storage changes and cumulative groundwater storage changes with respect to the storage on Nov. 1, 2011. Gray color represents the area of one standard deviation.

section CC′. Moreover, the seaward hydraulic gradient around the river is lower than the flood condition due to low pre-storm river stage that lasted more than one and a half months.

5.7.4. Groundwater responses to hurricane

Similar to the storm, a hurricane can also elevate groundwater head around the river and beneath the surrounding bays, but with much higher groundwater head. As shown in Fig. 12d, on August 29, 2012 groundwater head was estimated between 1.6 m and 2.8 m along the river and between 1.0 m and 2.8 m underneath the surrounding bays. High river and tidal stages lead to much higher groundwater recharge. Due to the track and counterclockwise rotation of the hurricane, storm surges significantly elevated water level in the upper right corner of the study site (the upper portion of the Breton Sound estuary) and caused significate elevation in the groundwater head (Fig. 12d).

5.8. Impact on factor of safety

The factor of safety was calculated using 30 realizations of model parameters at one of peak flood stages (February 15, 2012). As shown in Fig. 13a, several areas have more than 90% chance that the estimated factor of safety is lower than 1.5. The majority of the concerned areas are inside the ring levees, suggesting strong uplifting force acting on landside levee toes. The low factor of safety was due to high groundwater head either beneath a thin clayey blanket or in exposed sand. For example, at the cross section CC’ in Fig. 6b, a thin clayey layer can be seen in the eastern bank of Mississippi River and a blanket is missing in the western bank. Low factors of safety are shown in this cross section when river water is high. Fig. 13b shows areas with a factor of safety less than 1.5 at a lower river stage two weeks after the peak flood (March 1, 2012). The impacted areas are similar to the peak flood condition. This is because the levee-confined Mississippi River water produces groundwater level higher than land elevation in these areas.

The factor of safety was calculated using 30 realizations of model parameters at peak river and tidal stages (August 30, 2012) during Hurricane Isaac. As shown in Fig. 14a, areas with a factor of safety lower than 1.5 are smaller than the flood condition. This is due to storm surge elevates Mississippi River water and bay water, and creates a downward hydraulic gradient in most of the study area except areas within the ring levees. Fig. 14b shows much larger areas of having a factor of safety lower than 1.5 three days after the hurricane passed (September 2, 2012). This is because the retreating surface water removed overburdens, and caused reversed vertical hydraulic gradient at some areas outside the ring levees to experience uplifting forces. Fast reversion of hydraulic gradient along with high pore water pressure during and after hurricanes can threaten the ring levee systems as well as the coastal communities and industries in the MRD.

5.9. Groundwater implications

5.9.1. Infrastructure safety

Groundwater-surface water interactions in the MRD suggest a concern about infrastructure safety. For example, man-made river diversion can cause tens of meters of scouring in the diversion channel (Yuill et al., 2016). The scouring could alter subsurface hydrology by creating extra flow pathways for groundwater to interact with surface water, especially during severe hydrologic events. High pore water pressure could be delivered through the flow pathways to the foundations of infrastructures such as levees and river diversion complexes, thus could reduce effective stress of sediments and destabilize the foundation of structures (Nelson and Leclair, 2006; Sills et al., 2008). This mechanism may be intensified in a scenario when prolonged flooding overlapped with storms or hurricanes (Bilskie and Hagen, 2018). Further study is needed to evaluate this concern.

5.9.2. Salinization sand desalinization

As a river-deltaic system evolves under the influence of both river and sea, balance between fresh and saline water from these two sources drives variation in salinity in the delta (Fan et al., 2011). Surface-groundwater interactions in the MRD can fluctuate salinity in the groundwater system. River discharge to the groundwater system during flood months can reduce salinity in the sediments. However, the overwash process (Anderson, 2002; Terry and Falkland, 2010) associated with storms and hurricanes can bring saline water into the near-surface sediments. As a result, seawater intrusion to the groundwater system may harm vegetation, and result in wetland deterioration and elevation loss (Day et al., 2011; Shapouri et al., 2015).

5.9.3. Sediment erosion

High pore water pressure is one of the major mechanisms for enhancing sediment erosion by reducing effective stress in sediments (Robertson et al., 2007). Although groundwater simulation was conducted on a regional scale instead of a local scale resolution, this study suggests that high pore water pressure associated with severe hydrologic events is likely to destabilize sediments and enhance sediment erosion. Fine-grained sediments near the surface could migrate upward through seepage flow (Zhang et al., 2017). Areas experience significant

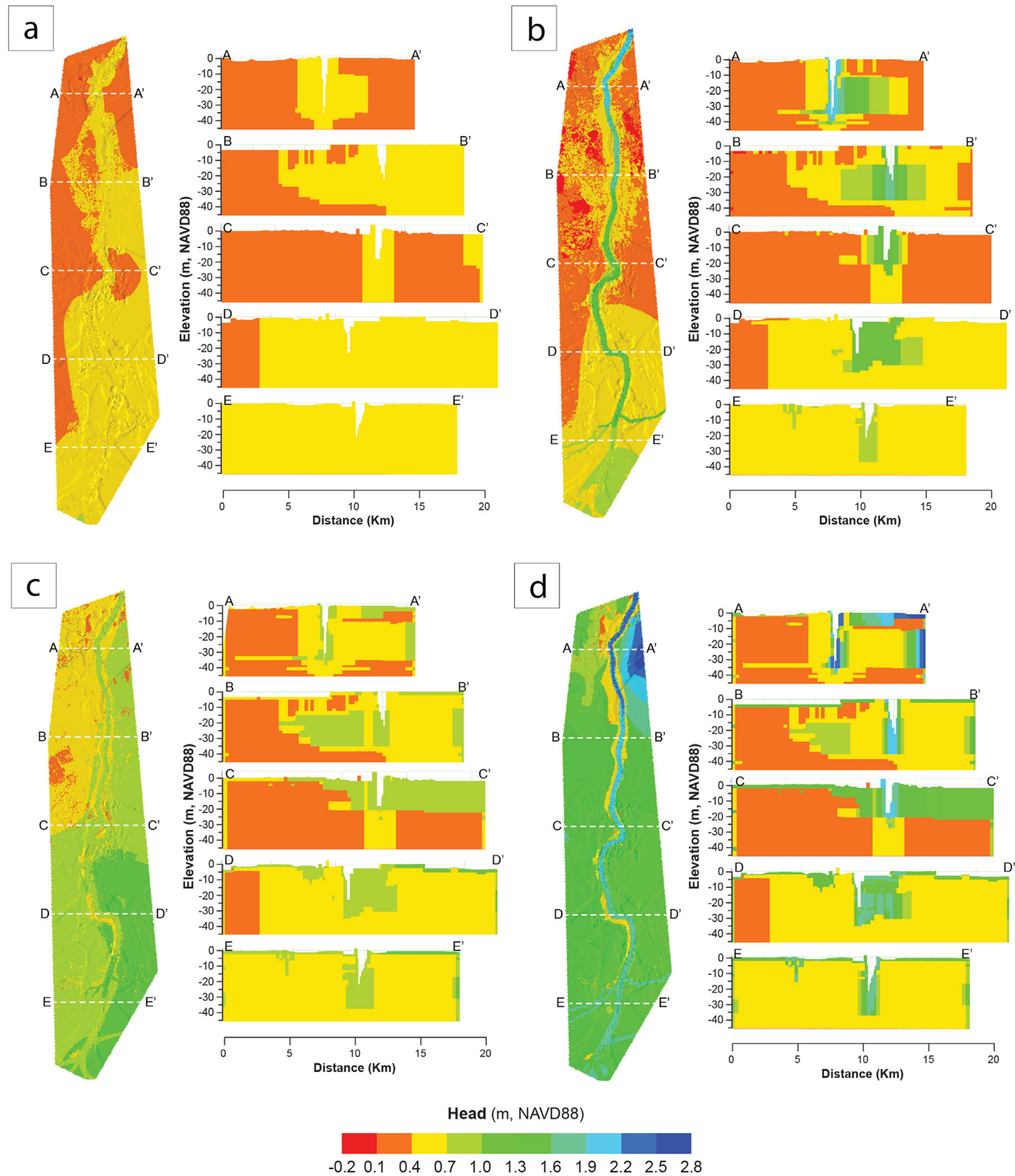

Fig. 12. Mean groundwater head distribution beneath topobathymetric surface and in the cross sections on (a) Nov.1, 2011, (b) Feb.11, 2012, (c) Jun. 24, 2012, and (d) Aug. 29, 2012. Dashed lines refer to the location of cross sections. All cross sections are vertically exaggerated by a factor of 120.

elevation in pore water pressure may become a hotspot for sediment erosion (Xu et al., 2016). Moreover, groundwater discharge associated with rapid drawdown of the surge water after hurricanes may also lead to momentary liquefaction (Sumer, 2002).

6. Conclusions

The major findings on the dynamics of groundwater flows in the Mississippi River delta (MRD) can be summarized as follows.

(1) This study reveals the complexity of the MRD hydrogeological setting in the top 50 m. Although the stratigraphy model shows a general clay-sand-clay layering in the MRD, the near-surface stratigraphy is complicated by sandy sediments deposited through splay channel in-fill, overbank flooding, and tributary extension. These sandy sediments can serve as preferential conduits for groundwater flow and form hotspots for exchanging and mixing of groundwater with bay water. Confined sands incised by the Mississippi River channel between −10 m and −35 m are main places where high pore water pressure is delivered from the river to the groundwater system.

(2) Groundwater discharge to and recharge from Mississippi River and the surrounding bays depend on local hydraulic gradients at the interfaces. Due to more frequent changes in inundation patterns and hydraulic gradients, the groundwater system exchanges more frequently with bays than with the Mississippi River. The estimated groundwater fluxes across the river and tide boundaries are in the magnitude of 10^5–10^6 m^3/day, which is three to four orders of magnitude less than the Mississippi River discharge rate. Although the groundwater fluxes are relatively insignificant, groundwater

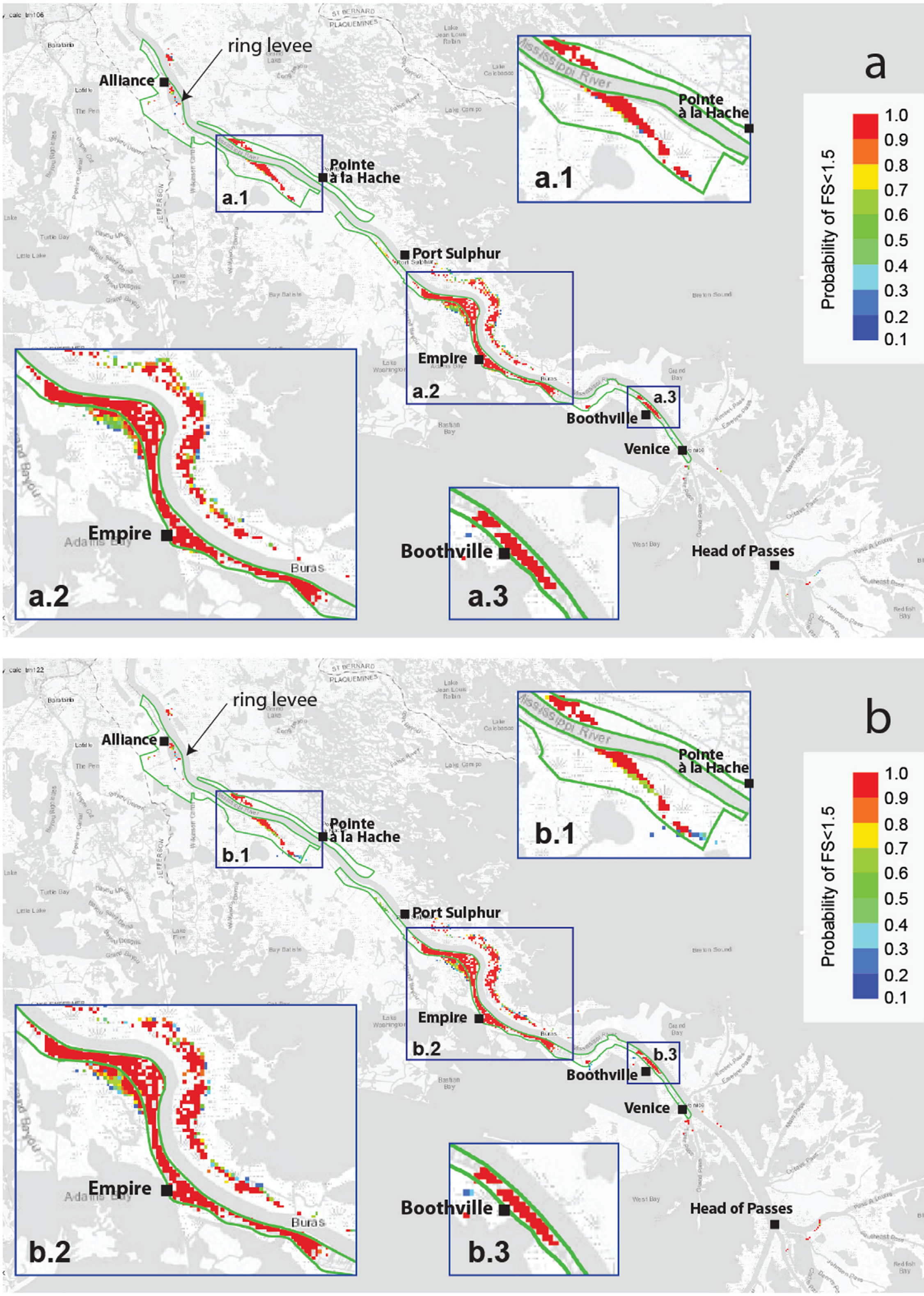

Fig. 13. Maps of probability of factor of safety less than 1.5 during flood: (a) at a peak flood stage (February 15, 2012), and (b) after the flood (March 1, 2012).

may play a significant role in exchanging and mixing with surface water and forming hotspots for biogeochemical processes.

(3) Dramatic groundwater head variation in the MRD can occur in sandy sediments and is closely associated with hydrologic events. Groundwater head is low and its distribution is relatively uniform across the MRD given a long pre-flood period. A long flood season can elevate pore water pressure around the river, but does not impact much groundwater head underneath the surrounding bays. Severe tropical storms and hurricanes can significantly elevate groundwater head in the MRD, especially in the areas experiencing the highest storm surges. Hurricanes are the most damaging players, which can elevate pore water pressure 4 times or more

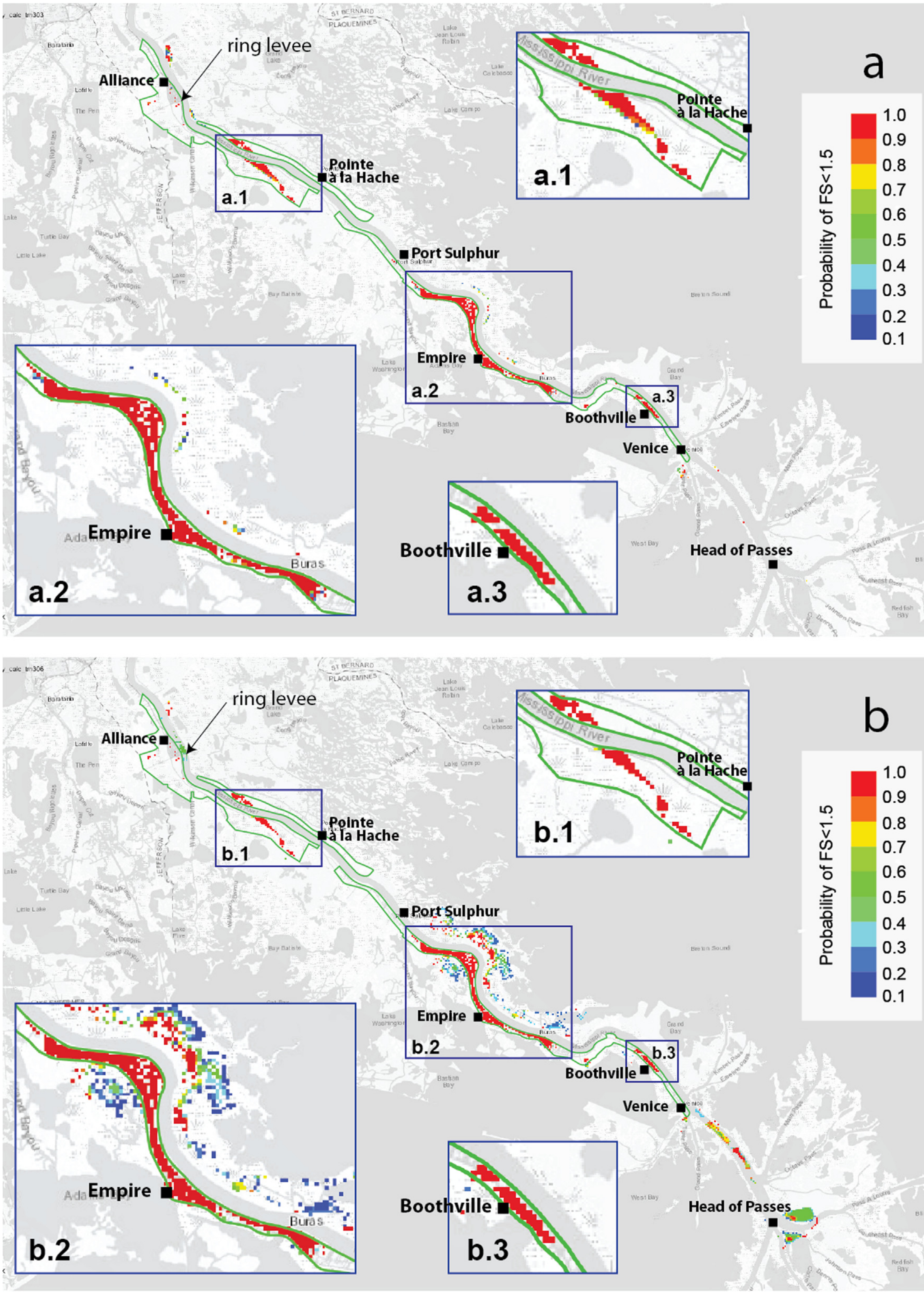

Fig. 14. Maps of probability of factor of safety less than 1.5 during Hurricane Isaac: (a) at groundwater recharge peak (August 30, 2012), and (b) at groundwater discharge peak (September 2, 2012).

higher than the normal condition within a few days. Groundwater recharge rate is at its peak during peak river and tide stages, but quickly drops and reverses to peak groundwater discharge rate a few days later after hurricanes pass.

(4) Groundwater-surface water interactions triggered by severe hydrological events such as floods and storms can significantly elevate groundwater heads and result in low factors of safety. A harmful condition can be created a few days later after a hurricane passes. This study discovers a sharp groundwater recharge-to-discharge reversion occurs right after hurricanes. Vertical hydraulic

gradient can be reversed quickly once the receding surface water removes the overburdens. The delayed groundwater response to receding surface waters can create a high upward hydraulic gradient to shallow sediments and larger areas with low factor of safety.

(5) This study suggests that high pore water pressure and low factor of safety during floods, storms, and hurricanes may compromise coastal infrastructures. High pore water pressure can reduce effective stress in sediments, weaken soil strength, destabilize sediments and enhance sediment erosion in coastal zones. This mechanism may be intensified in a scenario when prolonged flooding overlapped with storms or hurricanes. Further study is needed to evaluate this concern.

CRediT authorship contribution statement

An Li: Conceptualization, Methodology, Formal analysis, Investigation, Validation, Visualization, Writing - original draft, Writing - review & editing. **Frank T.-C. Tsai:** Conceptualization, Methodology, Investigation, Funding acquisition, Project administration, Supervision, Writing - original draft, Writing - review & editing.

Declaration of Competing Interest

The authors declare that they have no known competing financial interests or personal relationships that could have appeared to influence the work reported in this paper.

Acknowledgements

This project was funded by The Water Institute of the Gulf under project award number RCEGR260003-01-00 [CPRA-2015-COE-MB]. This project was paid for with federal funding from the Department of the Treasury through the Louisiana Coastal Protection and Restoration Authority's Center of Excellence Research Grants Program under the Resources and Ecosystems Sustainability, Tourist Opportunities, and Revived Economies of the Gulf Coast States Act of 2012 (RESTORE Act). The statements, findings, conclusions, and recommendations are those of the author(s) and do not necessarily reflect the views of the Department of the Treasury, CPRA or The Water Institute of the Gulf.

References

Allison, M.A., Demas, C.R., Ebersole, B.A., Kleiss, B.A., Little, C.D., Meselhe, E.A., Powell, N.J., Pratt, T.C., Vosburg, B.M., 2012. A water and sediment budget for the lower Mississippi-Atchafalaya River in flood years 2008–2010: implications for sediment discharge to the oceans and coastal restoration in Louisiana. J. Hydrol. 432, 84–97. https://doi.org/10.1016/j.jhydrol.2012.02.020.

Allison, M., Yuill, B., Törnqvist, T., Amelung, F., Dixon, T.H., Erkens, G., Stuurman, R., Jones, C., Milne, G., Steckler, M., Syvitski, J., 2016. Global risks and research priorities for coastal subsidence. Eos 97 (19), 22–27. https://doi.org/10.1029/2016EO055013.

Anderson, W.P., 2002. Aquifer salinization from storm overwash. J. Coastal Res. 18 (3), 413–420.

ASTM, 2017. D2487-17. Standard Practice for Classification of Soils for Engineering Purposes (Unified Soil Classification System). American Society for Testing and Materials, ASTM International, West Conshohocken, PA. DOI:10.1520/D2487-17.

Basu, A.R., Jacobsen, S.B., Poreda, R.J., Dowling, C.B., Aggarwal, P.K., 2001. Large groundwater strontium flux to the oceans from the Bengal Basin and the marine strontium isotope record. Science 293 (5534), 1470–1473. https://doi.org/10.1126/science.1060524.

Batu, V., 1998. Aquifer Hydraulics: A Comprehensive Guide to Hydrogeologic Data Analysis. John Wiley and Sons, New York.

Bentley, S.J., Blum, M.D., Maloney, J., Pond, L., Paulsell, R., 2016. The Mississippi River source-to-sink system: Perspectives on tectonic, climatic, and anthropogenic influences, Miocene to Anthropocene. Earth Sci. Rev. 153, 139–174. https://doi.org/10.1016/j.earscirev.2015.11.001.

Berg, R., 2013. Tropical Cyclone Report Hurricane Isaac (AL092012) 21 August–1 September 2012. National Hurricane Center.

Bianchi, D.T.S., Allison, D.M.A., Cai, P.W.-J., 2013. Biogeochemical Dynamics at Major River-Coastal Interfaces: Linkages with Global Change. Cambridge University Press, New York, NY.

Bilskie, M.V., Hagen, S.C., 2018. Defining flood zone transitions in low-gradient coastal regions. Geophys. Res. Lett. 45 (6), 2761–2770. https://doi.org/10.1002/2018GL077524.

Bomer, E.J., Bentley, S.J., Hughes, J.E., Wilson, C.A., Crawford, F., Xu, K., 2019. Deltaic morphodynamics and stratigraphic evolution of middle Barataria Bay and middle Breton sound regions, Louisiana, USA: implications for River-Sediment Diversions. Estuar. Coast. Shelf Sci. 224, 20–33. https://doi.org/10.1016/j.ecss.2019.03.017.

Burnett, W.C., Aggarwal, P.K., Aureli, A., Bokuniewicz, H., Cable, J.E., Charette, M.A., Kontar, E., Krupa, S., Kulkarni, K.M., Loveless, A., Moore, W.S., 2006. Quantifying submarine groundwater discharge in the coastal zone via multiple methods. Sci. Total Environ. 367 (2), 498–543. https://doi.org/10.1016/j.scitotenv.2006.05.009.

Cable, J.E., Burnett, W.C., Chanton, J.P., Weatherly, G.L., 1996. Estimating groundwater discharge into the northeastern Gulf of Mexico using radon-222. Earth Planet. Sci. Lett. 144 (3), 591–604. https://doi.org/10.1016/S0012-821X(96)00173-2.

Chamberlain, E.L., Törnqvist, T.E., Shen, Z., Mauz, B., Wallinga, J., 2018. Anatomy of Mississippi Delta growth and its implications for coastal restoration. Sci. Adv. 4 (4), eaar4740. https://doi.org/10.1126/sciadv.aar4740.

Chen, J., Taniguchi, M., Liu, G., Miyaoka, K., Onodera, S.I., Tokunaga, T., Fukushima, Y., 2007. Nitrate pollution of groundwater in the Yellow River delta, China. Hydrogeol. J. 15 (8), 1605–1614. https://doi.org/10.1007/s10040-007-0196-7.

Christopher, C.M., Oscar, K.H., Roberts, H.H., Liam, E.G., Menzel, W.P., 1993. Response of Louisiana coastal environments to a cold front passage. J. Coastal Res. 9 (2), 434–447.

Chuang, W.-S., Wiseman Jr., W.J., 1983. Coastal sea level response to frontal passages on the Louisiana-Texas shelf. J. Geophys. Res. Oceans 88 (C4), 2615–2620. https://doi.org/10.1029/JC088iC04p02615.

Coleman, J.M., 1988. Dynamic changes and processes in the Mississippi River delta. GSA Bull. 100 (7), 999–1015. https://doi.org/10.1130/0016-7606(1988)100<0999:DCAPIT>2.3.CO;2.

Coleman, D.J., Kolker, A.S., Johannesson, K.H., 2016. Submarine groundwater discharge and alkaline earth element dynamics in a deltaic coastal setting. Hydrol. Res. 48 (5), 1169–1176. https://doi.org/10.2166/nh.2016.285.

CPRA, 2012. Louisiana's Comprehensive Master Plan for a Sustainable Coast. 2012 Coastal Master Plan, Coastal Protection and Restoration Authority of Louisiana, Baton Rouge, Louisiana.

CPRA, 2017. Louisiana's Comprehensive Master Plan for a Sustainable Coast. 2017 Coastal Master Plan, Coastal Protection and Restoration Authority of Louisiana, Baton Rouge, Louisiana.

CPRA, 2018. Coastwide Reference Monitoring System. Coastal Protection and Restoration Authority of Louisiana. Available at: https://lacoast.gov/crms/. (accessed on 1 May 2018).

Day, J.W., Boesch, D.F., Clairain, E.J., Kemp, G.P., Laska, S.B., Mitsch, W.J., Orth, K., Mashriqui, H., Reed, D.J., Shabman, L., Simenstad, C.A., 2007. Restoration of the Mississippi Delta: lessons from Hurricanes Katrina and Rita. Science 315 (5819), 1679–1684. https://doi.org/10.1126/science.1137030.

Day, J.W., Giosan, L., 2008. Geomorphology: survive or subside? Nat. Geosci. 1 (3), 156–157. https://doi.org/10.1038/ngeo137.

Day, J.W., Kemp, G.P., Reed, D.J., Cahoon, D.R., Boumans, R.M., Suhayda, J.M., Gambrell, R., 2011. Vegetation death and rapid loss of surface elevation in two contrasting Mississippi delta salt marshes: the role of sedimentation, autocompaction and sea-level rise. Ecol. Eng. 37 (2), 229–240. https://doi.org/10.1016/j.ecoleng.2010.11.021.

Debnath, P., Mukherjee, A., 2016. Quantification of tidally-influenced seasonal groundwater discharge to the Bay of Bengal by seepage meter study. J. Hydrol. 537, 106–116. https://doi.org/10.1016/j.jhydrol.2016.03.010.

Domenico, P.A., Mifflin, M.D., 1965. Water from low-permeability sediments and land subsidence. Water Resour. Res. 1 (4), 563–576. https://doi.org/10.1029/WR001i004p00563.

Esposito, C.R., Shen, Z., Törnqvist, T.E., Marshak, J., White, C., 2017. Efficient retention of mud drives land building on the Mississippi Delta plain. Earth Surf. Dyn. 5, 387–397. https://doi.org/10.5194/esurf-5-387-2017.

Fan, X., Pedroli, B., Liu, G., Liu, H., Song, C., Shu, L., 2011. Potential plant species distribution in the Yellow River Delta under the influence of groundwater level and soil salinity. Ecohydrology 4 (6), 744–756. https://doi.org/10.1002/eco.164.

FEMA, 2015. Evaluation and Monitoring of Seepage and Internal Erosion, FEMA P-1032. U.S. Department of Homeland Security, Federal Emergency Management Agency, Interagency Committee on Dam Safety.

Feng, Z., Li, C., 2010. Cold-front-induced flushing of the Louisiana Bays. J. Mar. Syst. 82 (4), 252–264. https://doi.org/10.1016/j.jmarsys.2010.05.015.

Fisk, H.N., 1961. Bar-finger sands of Mississippi Delta. In: Peterson, J.A., Osmond, J.C. (Eds.), Geometry of Sandstone Bodies. American Association of Petroleum Geologists, Tulsa, Oklahoma, pp. 29–52.

Frazier, D.E., Osanik, A., 1969. Recent peat deposits-Louisiana coastal plain. Environments of Coal Deposition. Geol. Soc. Am. Spec. Pap. 114, 63–85.

Freeze, R.A., Cherry, A., 1979. Groundwater. Prentice-Hall Inc, New Jersey.

Guy, K.K., Stockdon, H.F., Plant, N.G., Doran, K.S., Morgan, K.L., 2013. Hurricane Isaac: Observations and analysis of coastal change, U.S. Geological Survey Open-File Report 2013–1270, 21p. DOI:10.3133/ofr20131270.

Harr, M.E., 1962. Groundwater and Seepage. McGraw-Hill, New York.

Helton, J.C., Davis, F.J., 2003. Latin hypercube sampling and the propagation of uncertainty in analyses of complex systems. Reliab. Eng. Syst. Saf. 81 (1), 23–69. https://doi.org/10.1016/S0951-8320(03)00058-9.

Hill, M.C., Cooley, R.L., Pollock, D.W., 1998. A controlled experiment in ground water flow model calibration. Groundwater 36 (3), 520–535. https://doi.org/10.1111/j.1745-6584.1998.tb02824.x.

Hogan, J.M., Van der Kamp, G., Barbour, S.L., Schmidt, R., 2006. Field methods for

measuring hydraulic properties of peat deposits. Hydrol. Process. 20 (17), 3635–3649. https://doi.org/10.1002/hyp.6379.
Hyfield, E.C., Day, J.W., Cable, J.E., Justic, D., 2008. The impacts of re-introducing Mississippi River water on the hydrologic budget and nutrient inputs of a deltaic estuary. Ecol. Eng. 32 (4), 347–359. https://doi.org/10.1016/j.ecoleng.2007.12.009.
Johnson, A. I., 1967. Specific yield – Compilation of specific yields for various materials. U.S. Geological Survey, Water Supply Paper, 1662-D. DOI: 10.3133/wsp1662D.
Junk, W.J., Bayley, P.B., Sparks, R.E., 1989. The flood pulse concept in river-floodplain systems. Can. Spec. Publ. Fish. Aquatic Sci. 106 (1), 110–127.
Kim, J., 2016. Investigating groundwater inputs to Mississippi River Deltaic wetlands using spatial and temporal responses of the geochemical tracer, 222 Rn. Thesis. The University of North Carolina at Chapel Hill.
Kimberlain, T.B., 2013. Tropical Cyclone Report: Tropical Storm Debby (AL042012) 23-27 June 2012, National Hurricane Center, January 7, 2013.
Knabb, R.D., Rhome, J.R., Brown, D.P., 2005. Tropical Cyclone Report: Hurricane Katrina 23-30 August 2005. National Hurricane Center, December 20, 2005.
Kolker, A.S., Cable, J.E., Johannesson, K.H., Allison, M.A., Inniss, L.V., 2013. Pathways and processes associated with the transport of groundwater in deltaic systems. J. Hydrol. 498, 319–334. https://doi.org/10.1016/j.jhydrol.2013.06.014.
Krest, J.M., Moore, W.S., Rama, 1999. 226Ra and 228Ra in the mixing zones of the Mississippi and Atchafalaya Rivers: indicators of groundwater input. Mar. Chem. 64 (3), 129–152. https://doi.org/10.1016/S0304-4203(98)00070-X.
Larson, J., Zhou, Y., Higgins, R.W., 2005. Characteristics of landfalling tropical cyclones in the United States and Mexico: climatology and interannual variability. J. Clim. 18 (8), 1247–1262. https://doi.org/10.1175/JCLI3317.1.
Leonards, G.A., 1962. Foundation Engineering. McGraw Hill, New York.
Letts, M.G., Roulet, N.T., Comer, N.T., Skarupa, M.R., Verseghy, D.L., 2000. Parametrization of peatland hydraulic properties for the Canadian Land Surface Scheme. Atmos. Ocean 38 (1), 141–160. https://doi.org/10.1080/07055900.2000.9649643.
Li, L., Barry, D.A., Stagnitti, F., Parlange, J.Y., Jeng, D.S., 2000. Beach water table fluctuations due to spring–neap tides: moving boundary effects. Adv. Water Resour. 23 (8), 817–824. https://doi.org/10.1016/S0309-1708(00)00017-8.
Li, A., Jafari, N.H., Tsai, F.T.-C., 2019. Modeling and comparing 3-D soil stratigraphy using subsurface borings and cone penetrometer tests in coastal Louisiana, USA. Georisk: Assessment and Management of Risk for Engineered Systems and Geohazards. DOI:10.1080/17499518.2019.1637528.
Li, A., Tsai, F.T.-C., Xu, K., Wang, J., White, C.M., Bentley, S.J., Chen, Q.J., 2019. Modeling sediment texture of river-deltaic wetlands in the Lower Barataria Bay and Lower Breton Sound, Louisiana, USA. Geo-Mar. Lett. 39 (2), 161–173. https://doi.org/10.1007/s00367-019-00566-2.
Liu, Y., Jiao, J.J., Liang, W., Luo, X., 2017. Tidal pumping-induced nutrients dynamics and biogeochemical implications in an intertidal aquifer. J. Geophys. Res. Biogeosci. 122 (12), 3322–3342. https://doi.org/10.1002/2017JG004017.
Liu, Q., Mou, X., 2016. Interactions between surface water and groundwater: key processes in ecological restoration of degraded coastal wetlands caused by reclamation. Wetlands 36 (1), 95–102. https://doi.org/10.1007/s13157-014-0582-6.
Love, M., Amante, C., Eakins, B., Taylor, L., 2010a. Digital elevation models of New Orleans, Louisiana: Procedures, data sources and analysis. National Geophysical Data Center, Marine Geology and Geophysics Division, Boulder, Colorado.
Love, M., Caldwell, R., Carignan, K., Eakins, B., Taylor, L., 2010. Digital Elevation Models of Southern Louisiana: Procedures, Data Sources and Analysis. National Geophysical Data Center, Boulder, Colorado.
McCoy, C.A., Corbett, D.R., McKee, B.A., Top, Z., 2007. An evaluation of submarine groundwater discharge along the continental shelf of Louisiana using a multiple tracer approach. J. Geophys. Res. Oceans 112 (C3), 1–13. https://doi.org/10.1029/2006JC003505.
Meselhe, E.A., Sadid, K.M., Allison, M.A., 2016. Riverside morphological response to pulsed sediment diversions. Geomorphology 270, 184–202. https://doi.org/10.1016/j.geomorph.2016.07.023.
Milliman, J.D., Meade, R.H., 1983. World-wide delivery of river sediment to the oceans. J. Geol. 91 (1), 1–21. https://doi.org/10.1086/628741.
Moore, W.S., Krest, J., 2004. Distribution of 223Ra and 224Ra in the plumes of the Mississippi and Atchafalaya Rivers and the Gulf of Mexico. Mar. Chem. 86 (3), 105–119. https://doi.org/10.1016/j.marchem.2003.10.001.
Narasimhan, T.N., Witherspoon, P.A., 1976. An integrated finite difference method for analyzing fluid flow in porous media. Water Resour. Res. 12 (1), 57–64. https://doi.org/10.1029/WR012i001p00057.
National Climatic Data Center, 2018. Climate of Louisiana. Available at: https://www.ncdc.noaa.gov/ (accessed on 1 May 2018).
National Weather Service, 2019. Hurricane Barry July 13, 2019. Available at: https://www.weather.gov/mob/barry. (accessed on 1 August 2019).
Nelson, S.A., Leclair, S.F., 2006. Katrina's unique splay deposits in a New Orleans neighborhood. GSA Today 16 (9), 4. https://doi.org/10.1130/GSAT01609A.1.
NOAA, 2018. Tides and Currents: Water Levels. National Oceanic and Atmospheric Administration. Available at: https://tidesandcurrents.noaa.gov/ (accessed on 1 May 2018).
NOAA, 2018. Vertical Datum Transformation. National Oceanic and Atmospheric Administration. Available at: https://vdatum.noaa.gov (accessed on 1 May 2018).
O'Connor, M.T., Moffett, K.B., 2015. Groundwater dynamics and surface water–groundwater interactions in a prograding delta island, Louisiana, USA. J. Hydrol. 524, 15–29. https://doi.org/10.1016/j.jhydrol.2015.02.017.
Panday, S., Langevin, C.D., Niswonger, R.G., Ibaraki, M., Hughes, J.D., 2017. MODFLOW–USG version 1.4.00: an unstructured grid version of MODFLOW for simulating groundwater flow and tightly coupled processes using a control volume finite-difference formulation. U. S. Geological Survey Software Release, 27 October 2017, DOI:10.5066/F7R20ZFJ.
Reading, H.G., 1978. Sedimentary Environments and Facies. Blackwell Science Ltd., Oxford.
Roberts, H.H., 1997. Dynamic changes of the Holocene Mississippi River delta plain: the delta cycle. J. Coastal Res. 13 (3), 605–627.
Robertson, P.K., Cabal, K.L., 2015. Guide to Cone Penetration Testing for Geotechnical Engineering. Gregg Drilling & Testing Inc., California.
Robertson, I.N., Riggs, H.R., Yim Solomon, C., Young Yin, L., 2007. Lessons from Hurricane Katrina storm surge on bridges and buildings. J. Waterw. Port Coastal Ocean Eng. 133 (6), 463–483. https://doi.org/10.1061/(ASCE)0733-950X(2007)133:6(463).
Santos, I.R., Burnett, W.C., Dittmar, T., Suryaputra, I.G., Chanton, J., 2009. Tidal pumping drives nutrient and dissolved organic matter dynamics in a Gulf of Mexico subterranean estuary. Geochim. Cosmochim. Acta 73 (5), 1325–1339. https://doi.org/10.1016/j.gca.2008.11.029.
Sawyer, A.H., Edmonds, D.A., Knights, D., 2015. Surface water-groundwater connectivity in deltaic distributary channel networks. Geophys. Res. Lett. 42 (23), 10–299. https://doi.org/10.1002/2015GL066156.
Shapouri, M., et al., 2015. The variation of stygofauna along a gradient of salinization in a coastal aquifer. Hydrol. Res. 47 (1), 89–103. https://doi.org/10.2166/nh.2015.153.
Shen, Z., Törnqvist, T.E., Mauz, B., Chamberlain, E.L., Nijhuis, A.G., Sandoval, L., 2015. Episodic overbank deposition as a dominant mechanism of floodplain and delta-plain aggradation. Geology 43 (10), 875–878. https://doi.org/10.1130/G36847.1.
Sibson, R., 1980. A vector identity for the Dirichlet tessellation. Math. Proc. Cambridge Philos. Soc. 87 (1), 151–155. https://doi.org/10.1017/S0305004100056589.
Sibson, R., 1981. A brief description of natural neighbour interpolation. In: Barnett, V. (Ed.), Interpreting Multivariate Data. John Wiley and Sons, New York.
Sills, G.L., Vroman, N.D., Wahl, R.E., Schwanz, N.T., 2008. Overview of New Orleans levee failures: lessons learned and their impact on national levee design and assessment. J. Geotech. Geoenviron. Eng. 134 (5), 556–565. https://doi.org/10.1061/(ASCE)1090-0241(2008) 134:5(556).
Storm Prediction Center, 2012. Storm Prediction Center Storm Reports for March 21 2012. Storm Prediction Center, National Oceanic and Atmospheric Administration.
Sumer, B.M., 2002. The Mechanics of Scour in the Marine Environment. World Scientific Publishing Company, Singapore.
Terry, J.P., Falkland, A.C., 2010. Responses of atoll freshwater lenses to storm-surge overwash in the Northern Cook Islands. Hydrogeol. J. 18 (3), 749–759. https://doi.org/10.1007/s10040-009-0544-x.
Thompson, C., Smith, L., Maji, R., 2007. Hydrogeological modeling of submarine groundwater discharge on the continental shelf of Louisiana. J. Geophys. Res. Oceans 112 (C3), 1–13. https://doi.org/10.1029/2006JC003557.
Törnqvist, T.E., Meffert, D.J., 2008. Sustaining coastal urban ecosystems. Nat. Geosci. 1, 805. https://doi.org/10.1038/ngeo365.
Tsai, F.T.-C., Sun, N.-Z., Yeh, W.W.G., 2005. Geophysical parameterization and parameter structure identification using natural neighbors in groundwater inverse problems. J. Hydrol. 308 (1), 269–283. https://doi.org/10.1016/j.jhydrol.2004.11.004.
USACE, 1956. Investigation of Underseepage and Its Control, Lower Mississippi River Levees. Technical Memorandum No. 3-434, U.S. Army Corps of Engineers, Army Engineer Waterways Experiment Station, Vicksburg, Mississippi.
USACE, 1992. Design, Construction, and Maintenance of Relief Wells. EM 1110-2-1914, U.S. Army Corps of Engineers, Washington, D.C.
USACE, 1993. Seepage Analysis and Control for Dams. EM 1110-2-1901, U.S. Army Corps of Engineers, Washington, D.C.
USACE, 2018. Water Levels of Rivers and Lakes. U.S. Army Corps of Engineers. Available at: http://rivergages.mvr.usace.army.mil (accessed on 1 May 2018).
USGS, 2018. National Water Information System. U.S. Geological Survey. Available at: https://waterdata.usgs.gov/nwis (accessed on 1 May 2018).
Welder, F.A., 1955. Deltaic Processes in Cubits Gap Area, Plaquemines Parish, Louisiana. Dissertation. Louisiana State University, Baton Rouge.
Wolski, P., Savenije, H.H.G., 2006. Dynamics of floodplain-island groundwater flow in the Okavango Delta, Botswana. J. Hydrol. 320 (3–4), 283–301. https://doi.org/10.1016/j.jhydrol.2005.07.027.
Xu, K., Mickey, R.C., Chen, Q., Harris, C.K., Hetland, R.D., Hu, K., Wang, J., 2016. Shelf sediment transport during hurricanes Katrina and Rita. Comput. Geosci. 90, 24–39. https://doi.org/10.1016/j.cageo.2015.10.009.
Xu, K., Bentley, S.J., Day, J.W., Freeman, A.M., 2019. A review of sediment diversion in the Mississippi River Deltaic Plain. Estuar. Coast. Shelf Sci. https://doi.org/10.1016/j.ecss.2019.05.023.
Younger, P.L., 1993. Simple generalized methods for estimating aquifer storage parameters. Q. J. Eng. Geol. 26, 127–135. https://doi.org/10.1144/GSL.QJEG.1993.026.02.04.
Yuill, B.T., Khadka, A.K., Pereira, J., Allison, M.A., Meselhe, E.A., 2016. Morphodynamics of the erosional phase of crevasse-splay evolution and implications for river sediment diversion function. Geomorphology 259, 12–29. https://doi.org/10.1016/j.geomorph.2016.02.005.
Zhang, S., Jia, Y., Wen, M., Wang, Z., Zhang, Y., Zhu, C., Li, B., Liu, X., 2017. Vertical migration of fine-grained sediments from interior to surface of seabed driven by seepage flows–'sub-bottom sediment pump action'. J. Ocean Univ. China 16, 15–24. https://doi.org/10.1007/s11802-017-3042-0.